JPL PUBLICATION 84-49

Spaceborne Receivers

Basic Principles

J.M. Stacey

December 1, 1984

NASA
National Aeronautics and
Space Administration

Jet Propulsion Laboratory
California Institute of Technology
Pasadena, California

JPL PUBLICATION 84-49

Spaceborne Receivers

Basic Principles

J.M. Stacey

December 1, 1984

NASA
National Aeronautics and
Space Administration

Jet Propulsion Laboratory
California Institute of Technology
Pasadena, California

The research described in this publication was carried out by the Jet Propulsion Laboratory, California Institute of Technology, under a contract with the National Aeronautics and Space Administration.

TABLE OF CONTENTS

BACKGROUND 1

SOME FIRST PRINCIPLES OF MICROWAVE RADIOMETRY 2

BASIC RADIOMETER TYPES 3

SOME IMPORTANT DEFINITIONS 15

THE TRANSFER FUNCTION AND SENSITIVITY OF THE TOTAL-POWER RADIOMETER . . 16

SIGNAL SUPPRESSION BY DETECTORS 30

THE TRANSFER FUNCTION AND THE SENSITIVITY OF THE MODULATED RADIOMETER . 32

THE INPUT CIRCUIT OF THE MODULATED RADIOMETER 38

OPERATIONAL INSIGHT OF A MODULATED RADIOMETER 45

A STATISTICAL INTERPRETATION OF TEMPERATURE RESOLUTION 63

COMMENTARY 69

REFERENCES 70

FOREWORD

The technical journals and archive bulge with spaceborne receiver measurements taken in the laboratory, in the test chambers, and in the ultimate environment of space. Some of the variations in these data are explained by the existing body of mathematical expressions -- some are not.

The accumulated data bases that are available for analyses are enormous, the sample sizes are large, and the data are accurately taken and recorded by serious and competent investigators. The test and performance records of many of these receivers have been retrieved, organized, and critically analyzed.

Over 100 separately identifiable receiver channels have been qualified for space in the environmental chambers at JPL alone...most have been launched into space.

Because the observed variations in the output responses of a large number of receivers importantly disagree with the equations that predict them, an attempt has been made to start with the measured and observed results and to reassess the mathematical expressions that purport to explain basic receiver performance. In some instances, the equations that explain and estimate receiver performance are rederived by reverting to the basic theory of detectors as they are affected by noise waveforms.

ACKNOWLEDGEMENT

It is abundantly clear and sufficient to say that the long-term, hands-on experience and counsel of

Jim (E. J.) Johnston

Frank T. Barath

Pete (F. G.) Olson

Fred S. Soltis

Walt (W. A.) Johnson

and

Richard S. Iwasaki

made this monograph possible.

ABSTRACT

This report is concerned with the underlying principles of operation of microwave receivers, as they are mainly intended, for space observations of planetary surfaces.

Considerable attention is given to the design philosophy of the receiver as it is applied to operate functionally as an efficient receiving system.

The principle of operation of the key components of the receiver is discussed and the important differences among receiver types are explained.

Some new, and needed, definitions are constructed to serve the purposes of the reader.

Mathematical expressions are derived that explain the operating performance and the sensitivity expectations for both the modulated and total-power receiver configurations. The expressions are derived from first principles and are developed through the important intermediate stages to form practicable and easily applied equations.

Many examples are given to illustrate the transfer of thermodynamic energy from point-to-point within the receiver.

The language of microwave receivers is applied statistics, and this discipline has been rigidly adopted to add precision and crispness to the interpretation of the derived quantities and to explain their uncertainties.

BACKGROUND

The basic principles of microwave radiometry as it is known today were first described in the technical literature by Dicke (Ref. 1) shortly after World War II. This radiometer concept, and the test instrument constructed to verify its performance, emerged from the MIT Radiation Laboratory as a fallout of the accelerated radar-receiver development program during the war years. Dicke's radiometer was modulated by a dipping-vane attenuator that was incorporated into a section of slotted waveguide that interconnected the mixer with a rectangular-horn antenna. The dipping-vane attenuator was driven at a 30-Hz rate by a synchronous motor that simultaneously served to synchronize a synchronous detector at the output of an amplitude detector. The dipping-vane attenuator introduced two new concepts: (1) the received signal temperatures were compared against a standard internal reference temperature (the vane temperature); and (2) the signal was modulated at the input of the receiver to differentiate it from the unmodulated internal noise generated by the receiver, i.e., mixer, RF components, amplifiers, and to allow it to be selectively sensed by the synchronous detector at the output of the detector. The combined effects operated to gain-stabilize the radiometer, albeit at a sacrifice to the overall sensitivity because the modulated receiver concept introduced several additional RF loss elements and essentially discarded one-half of the RF energy collected by the antenna.

Dicke s work with the modulated radiometer, however, was predated by other investigators who used simple superheterodyne receivers. Jansky observed sources of celestial emission that were interfering with radio transmission links. Reber constructed a radiometer and operated a radio astronomy facility on his own premises. Southworth (Ref. 2) observed the cosmic background, sun,

and crude blackbody sources with a double-superheterodyne receiver. Actually, Jansky, Reber, Southworth, and perhaps others, measured microwave fluxes with receivers that were only crudely gain-stabilized. These are truly the progenitors of the sensitive, gain-stabilized, total-power radiometer configuration as it is conceived today.

The heart of the instrumentation in a radio astronomy facility is the microwave radiometer. In fact, astronomy-related individuals and organizations have almost single-handedly been responsible for most of the major technical refinements incorporated in today's radiometric equipment. Commercial users and the military have only weakly adapted to microwave radiometer applications, probably because other more mature sensors and methods have been available.

The first microwave radiometer to operate successfully in space was carried by the Mariner II spacecraft for a flyby of Venus in 1962. In the early 1970's, observations of the Earth's surface and atmosphere were carried out by a series of microwave radiometers on board the Nimbus spacecraft and on Skylab. Other than Mariner II, a microwave radiometer has never been included among the complement of instruments on any spacecraft with a planetary mission.

At the onset of the 1980's, remote sensing of the Earth's atmosphere and surface from space emerged as a potentially useful but incompletely developed application for microwave radiometry. Ultimately, the disciplines most likely to benefit are: glaciology, hydrology, meteorology, and oceanography.

SOME FIRST PRINCIPLES OF MICROWAVE RADIOMETRY

A microwave radiometer is a system that receives and processes emitted radiation from matter at a physical temperature greater than zero kelvins (i.e., blackbodies and graybodies). The radiation may also be of the continuum

type or it may have spectral components such as with gases. A blackbody is defined as a radiator whose spectral emissivity is equal to 1 at all wavelengths and the radiation is randomly polarized. A graybody has the same characteristics as a blackbody except that the emissivity is less than 1 but is constant. A graybody may possess radiation components that are preferentially polarized in a matter of degree. Actually, the polarization properties of a graybody are better specified for the particular case. Conceptually a graybody is an imperfect blackbody.

As the name implies, the microwave radiometer is designed to operate in the microwave region of the spectrum with the understanding that sharp wavelength-boundaries are not well defined in terms of differentiating between radio, microwave, millimeter, and submillimeter wavelengths. For this reason the word "microwave" is intended to apply to all of those wavelengths in the sense that they share a common technology.

The microwave radiometer is conceived as a system because it employs analog and digital subsystems, RF assemblies, and temperature-calibration equipment. Among the most critical elements in the microwave radiometer design are the thermal and electrical features that stabilize the gain and execute accurate calibrations of signal intensities.

In general, microwave radiometers are not designed to respond to manmade emissions and, in fact, manmade emissions are usually categorized as interference.

BASIC RADIOMETER TYPES

The technical literature abounds with descriptions of various types of microwave radiometers that differ mainly in applications and in circuit

details. Fundamentally, however, all reduce to two basic types: total power and modulated. The principal difference between the two types is the manner in which the gains of the receiver components are stabilized.

The total-power radiometer employs sophisticated circuitry that is elaborately endowed with sensors and components that serve to maintain the overall receiver gain at a constant level during the measurement period. The gain stabilization methods of the total-power receiver are applied mainly to control amplitude variations in the power supply voltages and their AC-ripple components; also, the design of local oscillators, mixers, and all types of amplifiers in the overall amplification chain is amplitude stabilized to the highest possible degree. Feedback is introduced into the amplifier elements to stabilize the voltage gain and to maintain a stable bandpass response. Regeneration paths among amplifiers are rigidly minimized ... each amplifier is on a custom basis.

Gain stabilization is also introduced into the amplifier chains by incorporating compensating elements, such as thermistors, to compensate for longer-term gain changes caused by thermal stresses and gradients among the receiver components and chassis. In general, the gain must be stabilized for a period that is longer than the signal integration time and for the time occurring between calibration measurements. The postdetected radiometer output cannot distinguish between a change in the gain of an amplifier and a change in the signal intensity, because both appear as a change in the intrinsic receiver noise level. For this important reason, gain changes must always be suppressed to be a small fraction of the expected signal levels. It is of critical importance to realize that the signals received by the antenna system of a radiometer are noiselike in character and, except for their changes and amplitude peculiarities and signatures, are basically indistinguishable from

the internal receiver noise that is generated by the RF and IF components. Conceptually, and with the application of good design practice, the total-power radiometer is regarded as a simple device that offers good sensitivity. It operates well in both superheterodyne and tuned-radio-frequency (TRF) circuit configurations.

Modulated radiometers incorporate modulation processes that achieve gain stability by one means or another. Modulation is accomplished by RF-port switching, nulling, noise adding, waveguide-vane dipping, or using episcotisters, all serving the same purpose. Some, if not all of the methods, produce compromises in receiver sensitivity by the introduction of loss elements and components into the front end of the receiver. Signal energy losses are also caused by RF-port switching where the input signal is periodically disconnected (from the antenna) to compare its signal intensity with an internal temperature standard such as a blackbody radiator or a calibrated noise source. Gain stability must be consistently maintained in all the receiver components intervening between the front end and the synchronous detector at the output of the receiver.

The distinction between modulated and total-power radiometers is not always obvious. In certain radiometer configurations it is a moot point as to whether the input circuits of the radiometer are purposefully modulated to achieve gain stability or whether the modulation occurs as a requirement or as a consequence of the observing mode. A case in point is where multiple antenna beams are periodically switched at the input of the radiometer to compensate for atmospheric effects during an observation. In ground-based radio astronomy, for example, the antenna beam is periodically switched from the signal source to several nearby calibration sources (including the cosmic background) which in a sense serves to simultaneously calibrate the observations

and to suppress or minimize the temperature instabilities of the atmosphere. One can also envision the case where a total-power radiometer is required to periodically - and sometimes rapidly - switch its input from the antenna port to view an external calibration target. In this configuration, the total-power radiometer starts to assume some of the properties of a modulated radiometer. Up to this point in the discussion the distinction between total-power and modulated radiometers has been considered only in the most general and comparative terms. It is time to be more specific.

The circuit configurations of a total-power and a modulated radiometer are illustrated, by example, in Figs. 1 and 2. Both are shown as superheterodyne configurations. Either concept is adaptable to a TRF configuration where the mixer and the oscillator are eliminated and all predetection amplification is achieved at the received RF frequency.

A brief description of the two radiometer types shown in Figs. 1 and 2 seems appropriate. Both are included on the same panel to simplify comparisons.

In many remote-sensing applications, from orbit, there is an increasing trend to combine many radiometer channels into a single instrument enclosure and to even share a common multifrequency feed and antenna reflector. Multichannel radiometer configurations are mainly designed to extend the range of the geophysical parameters that can be observed in both the atmosphere and the surface. Combinations of two or more channels are also frequently combined to better explain the variations in parameters under investigation. For this reason the radiometer configurations shown in Figs. 1 and 2 are intended to illustrate one channel of many possible channels that may be contained within the same instrument enclosure. Notably, the figures allow that the illustrated

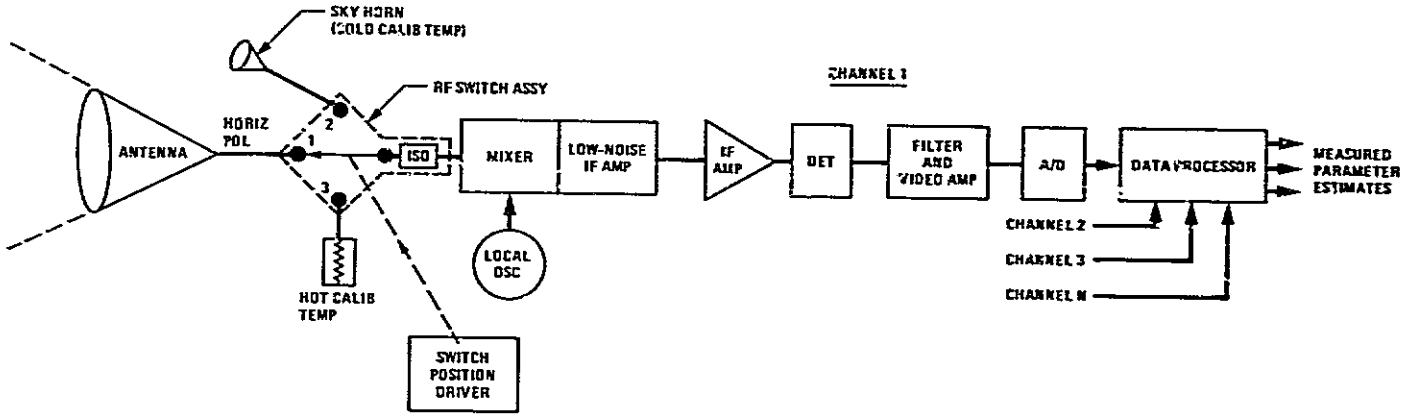

Fig. 1. Total-power radiometer system superheterodyne configuration single-frequency, single-polarized channel

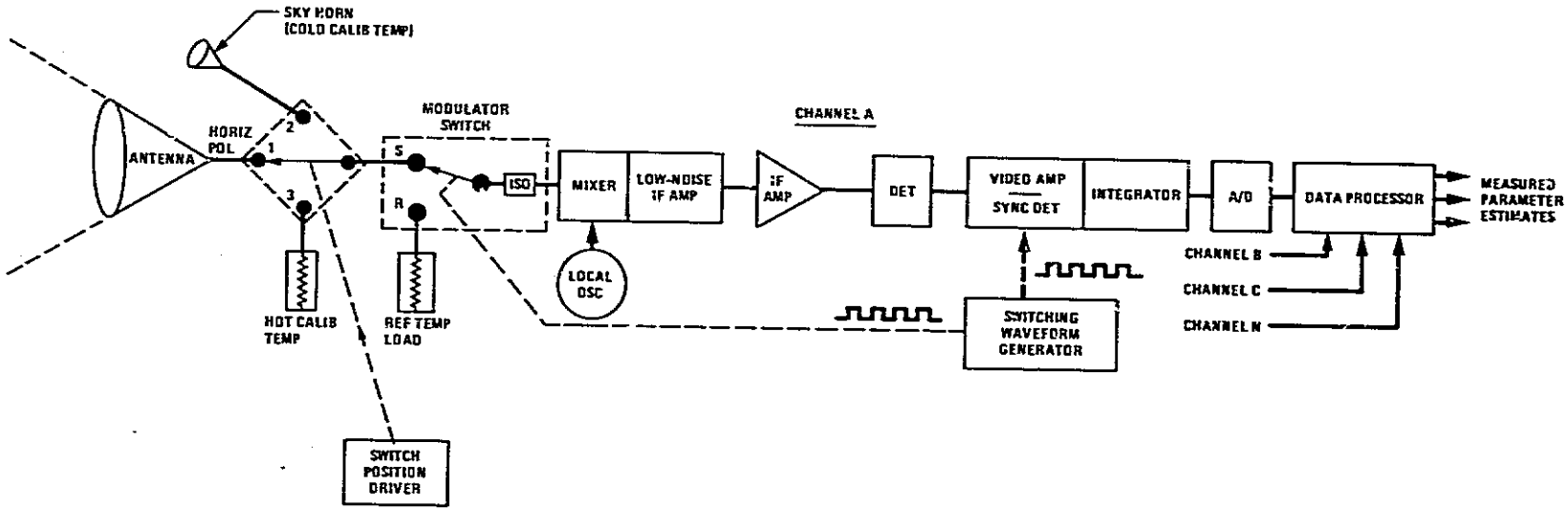

Fig. 2. Modulated radiometer system superheterodyne configuration single-frequency, single-polarized channel

configuration is only one of N channels. The data processor combines all the output responses from the N channels and directs them to the spacecraft telemetry system.

In the elementary and simple radiometer configurations shown in Figs. 1 and 2, attention is directed to the similarities and the differences between them. Each is shown to contain an identical calibration unit whose port positions are under the selective control of a switch position driver. In these figures the three port positions of the calibrator switch permit (1) an antenna or signal position, (2) a sky calibration horn position, and (3) a hot calibration temperature source observation. The switch position driver is normally included as part of a programmer unit that serves as a command unit, controlling and sequencing all operational functions of the radiometer itself. The sky horn is mainly symbolic as a cold calibration source. Other cold calibration sources may include (1) a radiatively cooled microwave load, (2) a blackbody radiator immersed in a cryogen, or (3) a blackbody target whose stabilized thermal temperature is only a few tens of degrees lower than the hot calibration temperature. The applicability of each depends upon the practicabilities of the observing situation.

Modulated radiometer configurations have long dominated the preferences of designers and users because, in the past, gain stability problems associated with total-power radiometers seemed intractable to solve. Mainly, the gain stability of total-power radiometers was significantly affected by: low-frequency ripple components in the power supplies; minute and variable regeneration propensities in the amplifiers; and mechanical stresses in the chassis and physical structure of the assembly caused by gravity as the orientation changed on the antenna support platform. Batteries were sometimes, and still are, used to circumvent some of the power supply voltage instabilities, but

they too can introduce new and peculiar problems, especially with the onset of aging and as the internal impedances change with use and time. And always there are gain variations caused by thermal stresses of the components and the mechanical structure. More recently, however, with the availability of solid-state components and superior circuit designs, many of the previous gain-stability problems associated with earlier radiometers (e.g., vacuum tubes, poorly stabilized power supplies, etc.) have significantly vanished. The total-power radiometer has become much more tractable with time.

Returning again to the discussion of Figs. 1 and 2: the hot calibration load as shown may be heated to a desired temperature or may, in fact, operate only at ambient temperature. In either, or any, case the load material is abundantly furnished with temperature sensors whose combined outputs report the exact temperature of the load material and show the occurrences of thermal gradients within it. Two calibrated temperatures are normally sufficient to establish a temperature slope-factor against which the signal temperatures are referenced.

The calibration switch itself is symbolic as shown here. In certain cases there is no switch at all. When an antenna or its feed assembly is sufficiently small and is connected directly to the isolator, in the total-power radiometer, or to the terminal "S," in the modulated radiometer, the antenna may be pointed directly at any of several external calibration sources. This latter method may enormously simplify a calibration requirement, and also reduce the number of lossy RF components that are associated with calibration, but it is not always practicable to do so.

The isolator that is shown connected to the input port of the mixer serves several purposes. Mainly, the isolator functions as an impedance matching device to compensate for mismatches (VSWR differences) between the mixer and the

components that precede it. Further, the isolator operates to prevent the leakage energy from the local oscillator (and its harmonics) from being reflected back into the front end of the radiometer. In this role, the isolator serves a vital function in the case of the modulated radiometer. Recent trends in mixer designs require high local-oscillator drive levels for efficient low noise operation of the mixer diodes. The higher local-oscillator drive levels, however, cause the diodes to produce strong higher-order harmonics of the local-oscillator frequency, which may be transmitted in the direction of the modulator switch where the harmonics are further modulated at the switching rate and accepted as bona fide signal components in the receiver bandpass. For these reasons the isolator is an important component and requires careful selection and adjustment to ensure a properly operating radiometer system while still maintaining the lowest possible RF losses. Moreover, the radiometer designer may be constrained to suppress the magnitude of the local oscillator and its harmonics from being radiated from the antenna or feed assembly. Local oscillator suppression is invoked when the fundamental oscillator frequency or any of its harmonics or cross products may interfere with companion sensors on the same spacecraft or when low-level radiation from the antenna becomes a consideration for any reason. Sometimes it is convenient and feasible to design the isolator such that it will reconcile the requirements for good radiometer operation and also to introduce a satisfactory level of attenuation to reduce the spurious radiation from the antenna originating in the local oscillator.

Again from Figs. 1 and 2, the components comprising the (1) low-noise IF amplifiers, (2) post-IF amplifiers, (3) detector, and (4) video amplifiers share a commonality for both radiometer types. Modern design practice tends to incorporate the low-noise amplifier with the mixer design.

The modulator switch, switching waveform generator, and synchronous detector are peculiar to the modulated radiometer. For purposes of discussion here, and elsewhere in this monograph, only the square wave switching waveform is considered because it features the waveform with best overall radiometer performance. Simultaneously, the switching waveform synchronizes the modulator switch and the synchronous detector. Here it is patently clear that the switching waveform operates on a 50 percent duty cycle as it alternately positions the input terminals of the modulator switch between the antenna port (or calibration temperatures) and the internal reference temperature load. It is also apparent that the signal is viewed only half of the time. The switching waveform characteristically operates at a rate that is consistent with the switching speeds of the modulator switch itself, with the further consideration that the switching rate will not occur at a harmonic of some lower waveform such as the power line frequency. In typical applications, 1000 hertz is commonly adopted as a convenient and practicable switch rate. At the very short millimeter wavelengths the switching rate may be reduced to only a few hertz to accommodate mechanical switches or ferrite devices with limited switching capabilities. The integration time for the observation influences the switching rate. That is, the signal must be sampled a sufficient number of times during the integration period to satisfactorily report the observed signal temperature. When an antenna beam is required to scan very rapidly over the Earth`s surface, for example, and the footprint dwell time is very short, a

higher switching rate may be required to permit a sufficient number of samples of the signal to be accumulated during the dwell-time of the footprint.

In the modulated radiometer the modulation principle operates to separate the signal component from the noise or bias components. The signal is, in fact, modulated at the switching rate and similarly demodulated by the synchronous detector.

In the total-power radiometer (Fig. 1) the integration of the signal is accomplished in the data processor after the analog-to-digital conversion. In the modulated radiometer, the integration is characteristically performed by circuitry following the synchronous detector.

The basic elements of the total-power and the modulated radiometer systems are also illustrated in functional form in Figs. 1 and 2. Both are shown as superheterodyne configurations. Either concept is adaptable to a tuned-radio frequency (TRF) type where the mixer and local oscillator are eliminated and all amplification is achieved at the received RF frequency.

Until recently, the total-power radiometer had not gained widespread acceptance among the microwave community because of the difficulties and problems with gain stabilization, even though the total-power radiometer is more sensitive than modulated radiometers by a theoretical factor of two. New developments in gain-stable solid-state amplifiers and low-ripple power supplies, together with more urgent needs for greater sensitivity, have motivated new interests in the total-power concept. Actually, the sensitivity of the total-power radiometer is improved over the modulated radiometer in some instances by better than a factor of two because the modulator switch and its RF loss are eliminated. In Figs. 1 and 2, the isolator that precedes the mixer is sometimes questioned as a necessary component. Actually, it mainly serves to compensate for imperfect matching (VSWR's > 1) among the RF components. It

is included here to prevent the leakage energy of the local oscillator and its harmonics from being reflected into the radiometer by the front-end RF components (i.e., switch antenna, waveguides, mixer, etc.).

In most applications where radiometers are employed there are requirements for internal calibration sources which serve to permit temperature comparisons of the signals with a temperature standard. Internal calibration devices such as hot waveguide terminations, noise diodes, or gas discharge tubes are commonly used. Hot terminations are usually placed in the end sections of waveguides or coaxial lines. They are fabricated from lossy materials such as carbon or graphite and within them are imbedded resistance wires which are electrically heated to accurately controlled temperatures and monitored by thermometer elements which are similarly imbedded within the lossy material. Usually the terminations are tapered or formed in a manner to optimally effect an impedance match with the incident fields within the waveguide or coaxial line.

Within certain wavelength intervals of the microwave and millimeter wave spectrums noise diodes are frequently used as a calibration device. Certain categories of semiconductor diodes produce high stable temperatures when DC currents are passed through them in the reverse direction.

Blackbody targets that are viewed by the antenna system or the feed assembly directly are frequently used for calibration. The blackbody targets take on the shape of disks, inverted pyramids, cones, and sometimes just a simple black box with a receiving aperture. The temperatures of these blackbody targets must be uniformly controlled and monitored by multiple thermometer elements that are distributed throughout the blackbody structure. Because they

have an emissivity that closely approximates a numerical value of 1 the thermometric temperature and the radiated temperature are, for all practicable purposes, assumed to be identical.

In some instances the antenna for the radiometer is implemented as a conical horn or as a standard-gain horn. For these antenna configurations an external calibration temperature source can be effected when an identical horn is mated aperture-to-aperture with an identical horn that is precisely terminated in a connecting waveguide section with a blackbody waveguide termination. The termination may be variably heated by resistance elements and monitored by thermometer elements. This type of calibration source requires an excellent match at the junction of the mating horn apertures and when this match is successfully implemented, in practice, the calibration source has the advantage of minimizing or even eliminating all significant spillover from sidelobes.

Basically, calibration is incorporated into the radiometer to monitor its sensitivity and gain stability. Some types of algorithms and software subroutines also require direct entries of the hot and cold calibration responses of the instrument into the equations that estimate the measured parameters. Mathematical expressions that are produced to relate the output responses of the radiometer instrument to the brightness temperatures of the wavefront appearing at the feed aperture are sometimes called temperature transfer functions. We should be continually aware that the radiometer actually measures the power density of the wavefront appearing at the collecting aperture in units of watts/m^2 and that this quantity is sometimes mathematically transformed into other units such as thermodynamic temperature only as a matter of convenience to certain categories of users.

The temperature transfer function (TTF) is the mathematical form that accurately expresses the signal input and output relationships of the radiometer. It is derived during the calibration process where its functional intent is to accurately estimate the temperature of the radiation viewed by the antenna beam, based on the output responses (digital or analog) of the radiometer. The mathematical terms of the temperature transfer function include the signal output responses of the radiometer and the output responses to the hot and cold calibration media. The end expectation of the temperature transfer function is to produce an accurate estimate of the radiative-body calibration target temperatures appearing within the antenna beam (commonly placed at the feed aperture), given only the output responses of the radiometer and certain specified internal monitoring media, such as RF component temperatures and calibration source variations.

The radiative-body temperature estimates given by the function must contain accountability for all potential nonlinear operations over the full range of target temperatures over the thermal operating range of all the radiometer components. Ultimately, the temperature transfer function is employed to certify the absolute accuracy of the radiometer (Ref. 4).

SOME IMPORTANT DEFINITIONS

The most important specifications affecting a radiometer system are the temperature resolution (Ref. 3) and the absolute accuracy (Ref. 4). The temperature resolution is a measure of how small a change in the antenna temperature is observable in the presence of internal receiver noise. The absolute accuracy expresses both the accuracy and the precision of the calibration.

There is no formalized agreement concerning the definition of absolute temperature accuracy as related to radiometry specifically, and much confusion and misunderstanding arises from this. An attempt is made here, however, to elucidate the point. The dart-board model shown in Fig. 3 serves to illustrate the concept of accuracy and precision in a sense that is only indirectly related to radiometry. The bull's eye expresses the true blackbody temperature of the calibration body and it is assumed to have no significant error because its calibration is presumed to be traceable to a certified primary temperature standard. With the use of the temperature transfer function the true temperatures of the calibrated targets are estimated over the total calibration-temperature range, and over the range of environmental conditions to which the radiometer is subjected. The matrix of residual errors that is generated provides the database from which the absolute temperature accuracy is calculated. The mean value of the residual errors expresses the accuracy of the systematic error given by the temperature transfer function. The standard deviation of the residual errors expresses the precision of the measurement and the statistical scatter in the sense that these errors cannot be calibrated.

THE TRANSFER FUNCTION AND SENSITIVITY OF THE TOTAL-POWER RADIOMETER

The basic elements of the total-power radiometer are shown schematically and functionally in Fig. 1 complete with a typical method of introducing calibration and data handling. In its simplest form, the total-power radiometer consists of a collecting aperture and a detector that are interconnected by low-noise amplifiers. Calibration devices, frequency converters, and data handling circuits are incorporated as conveniences to expedite the observations

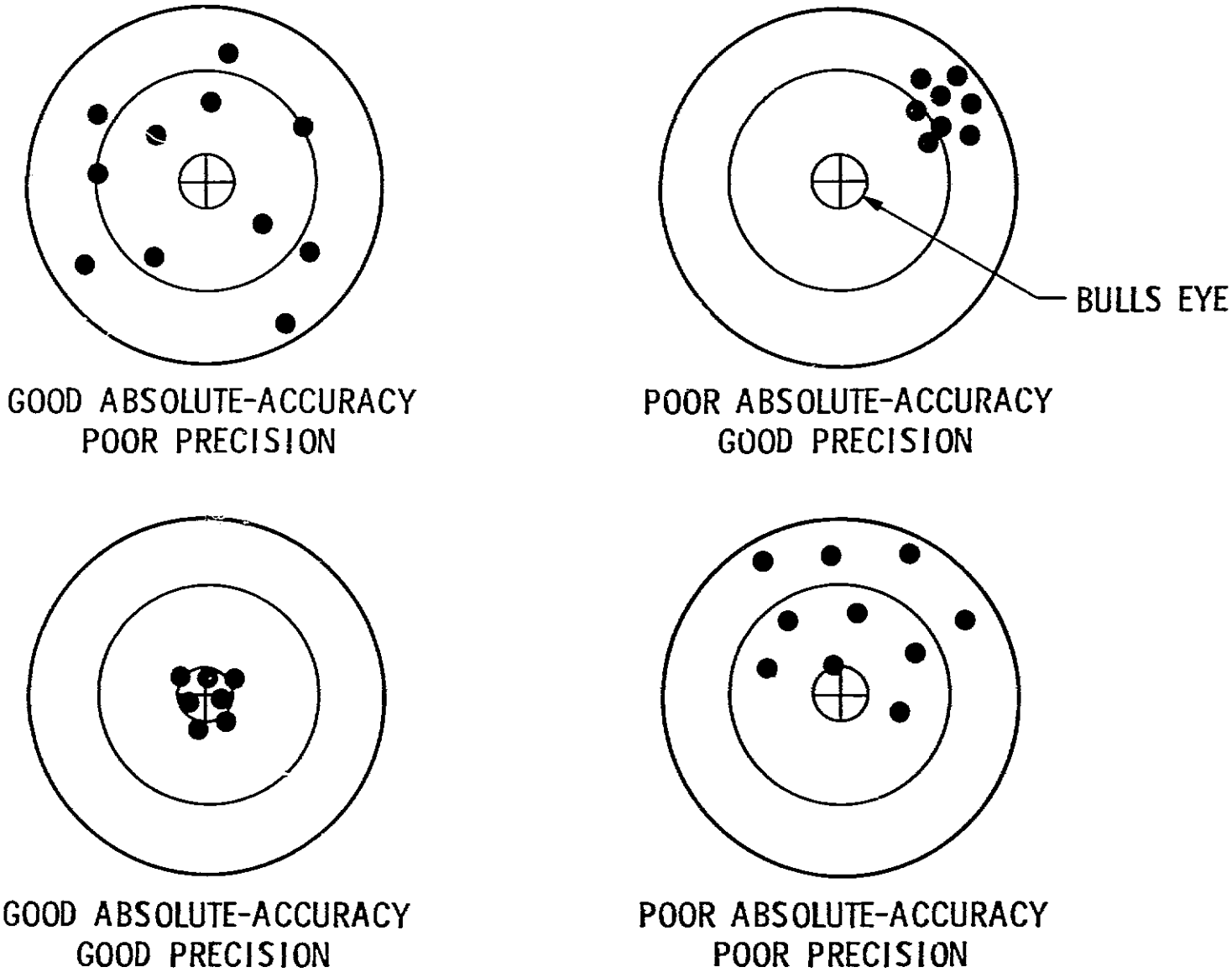

Fig. 3. Dart-board model of accuracy and precision

and improve the accuracy. With the exception of the detector, all radiometer components are defined to be linear and to remain linear within the operating constraints and specifications controlling the radiometer design. Good design practice requires that these components not be operated in an overloaded condition that will affect the symmetry of the amplification. Good radiometer design procedures also impose the requirement that any combination of signal-plus-internal-receiver noise will not produce nonsymmetrical amplification within the specified operating range. The linearity and symmetrical specifications similarly apply to the circuitry and data handling elements following the detector.

With the foregoing considerations and constraints the detector remains the single nonlinear element in the radiometer configuration.

The performance of the detector is most rigorously investigated and best understood by its dynamic input and output signal-to-noise relationships. A key characteristic that controls the operation of the detector is that the output signal-to-noise ratio is always less than unity. The mathematical structure of the signal and noise transfer characteristics of the detector will clearly show this in later paragraphs. When the noise at the input of the detector approaches zero, the output signal-to-noise approaches 1. By definition, the input signal is the component of the total noise power at the input to the detector, and within the predetection bandwidth, that varies in some consistent relationship with the power density changes in the wavefront appearing at the collecting aperture of the antenna. Further, it is presumed that the power-density changes in the wavefront are caused by variations in the observed phenomenon that is uniquely identifiable as the signal source. When

an earth-orbiting radiometer executes a drift-scan across a strong radio star, for example, the change in the noise power at the input to the detector is clearly and unambiguously proportional to the signal power.

What has actually occurred is that the radiance (signal) from the radio star has produced an increase in the power density of the wavefront at the collecting aperture and the receiver has transformed this increased power level into a change in the total power of the noise waveform appearing at the input of the detector. Notably, the non-stationary signal statistics are clearly distinguishable from the stationary statistics of the internal receiver noise within the predetection bandwidth.

It is relevant to mention here that the operating bias level of the detector is set by the internal receiver noise and that the relative power levels of the signal and internal noise can importantly affect the transfer characteristics of the detector, especially when the signal power starts to approach the internal receiver noise power. For astronomical observations, from earth orbit (excluding the sun and the moon) the signals are sufficiently small that they insignificantly affect the predetection noise levels set by internal receiver noise. For earth-surface observations from earth orbit, however, the radiances from the thermal gradients on the surface in combination with the radiances from atmospheric constituents such as dense clouds and rain can frequently produce composite signal components whose power levels significantly approach the internal noise level of the receiver at the detector.

The input noise to the detector is defined as that component of the total power contained within the predetection bandwidth that is generated internal to the radiometer by its circuits and losses and its power level remains constant.

If the internal receiver circuits introduce noise components that are modulated with any waveform, however small, they become indistinguishable from signal components.

Mainly, the noise power that is generated in the low-noise device that precedes the RF (or IF) amplification chain dominates the magnitude of the noise power at the detector input. Dissipative losses, preceding the low-noise device, make additional contributions. The signal power at the input of the detector is mainly influenced by the signal amplitude, its fluctuations, and by the predetection circuit losses.

The transfer function that expresses the input-output signal-to-noise ratios with no post-detection filtering is given by

$$\frac{S_o}{N_o} = \left[\frac{S_i}{S_i + N_i}\right]^2 = \frac{S_i^2}{(S_i + N_i)^2}$$

$$= \frac{S_i^2}{S_i^2 + 2S_iN_i + N_i^2} \qquad (1)$$

where S_i, S_o, N_i, and N_o sym' lize the input and output signal and noise powers (Refs. 8, 9, 10, 11).

Equation (1) explicitly shows that S_o/N_o, in all <u>practical</u> cases, is always less than unity, regardless of the input signal-to-noise relationships. Conceptually, the signal power always enters as a varying fraction of the total noise input given by the denominator.

The impact of the transfer function is plotted qualitatively in Fig. 4 to elucidate its general properties as a function of several ν^{th} law detectors (Ref. 6).

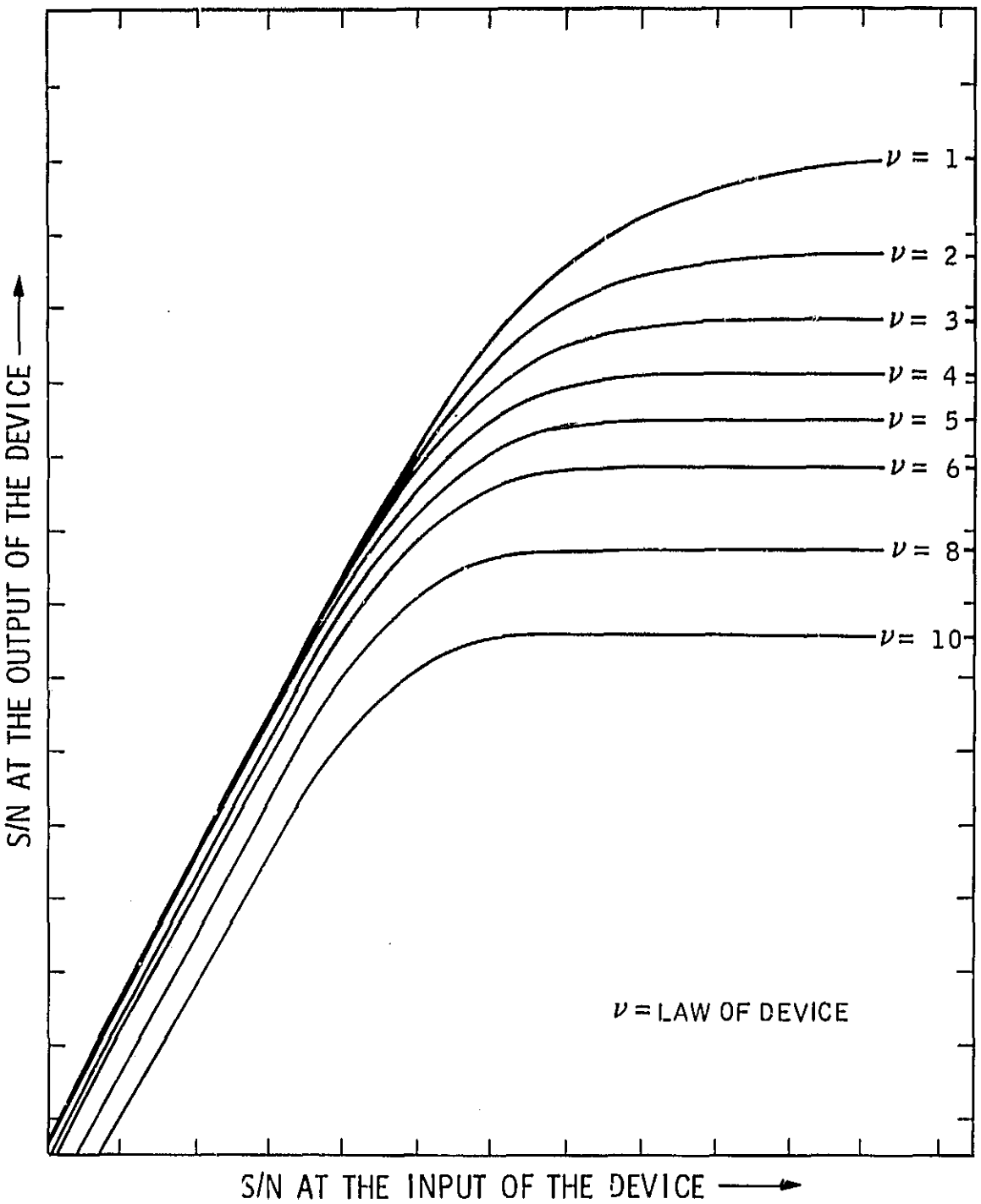

Fig. 4. Detector response characteristics, noise signal in receiver noise. (Adapted from Stone and Middleton, Ref. 6.)

Apparently, the input/output signal-to-noise ratios tend toward an amplitude compression for any exponent assigned to the detector. Moreover, all practical detectors (linear, square, cubical, etc.) tend to converge to approximately the same slope and amplitude as the square-law detector transfer function when the S/N at the input of the detector is very small - a consideration of interest when one is evaluating the relative properties and merits of different types of detectors. It is of singular importance to understand that the portions of the detector responses that exhibit very small slopes (saturation) at high input signal-to-noise ratios are produced by the intrinsic properties of the detector itself and are not caused by voltage limiting or other properties of the circuits that precede or follow the detector element itself. The plots shown in Fig. 4 are representative of the case where a narrow-band noise signal is immersed in narrow-band receiver noise, and where the bandwidth criterion is expressed by the ratio of the predetection bandwidth to the RF center-frequency. Microwave radiometers typically operate with narrow-band noise signals in narrow-band noise. For the typical operating condition, where the internal receiver noise power in the predetection bandpass is large compared to the signal power in the predetection bandpass, the detector produces its own operating bias from the internal receiver noise level.

The input noise-signal power S_i also enters into the denominator of (1) as a component of the total noise term $(S_i + N_i)^2$. Theoretically, this arises because of the cross-multiplication action of the input noise N_i with the signal. When the signal S_i and the internal receiver noise N_i are applied to the detector input, the resulting waveform is simply the vector sum of their instantaneous amplitudes. But because of the intrinsic nonlinearity of the detector, higher order harmonics and cross products are produced which

importantly modify the signal and noise relationships. Cross-multiplication terms are produced from $(S_i \times S_i)$, $(S_i \times N_i)$, and $(N_i \times N_i)$ which modify the well-defined system noise and signal components that entered the detector. In fact, these interactions actually produce noise products, at the expense of the signal energy, that render them indistinguishable from receiver noise.

If a filter is added to the output of the detector that samples the output waveform, with N degrees of freedom (independent samples) which are taken in a period of time equal to the reciprocal of the predetection bandwidth $1/B_{if}$ seconds apart, for the duration of the integration period, then the transfer function given in (1) is modified and recast as

$$\frac{S_o}{N_o} = (\tau B_{if}) \left[\frac{P_i}{P_i + N_i}\right]^2$$

or (2)

$$= \frac{B_{if}}{b_{pd}} \left[\frac{P_i}{P_i + N_i}\right]^2$$

where the time constant τ of the postdetection filter is recast in its equivalent postdetected bandwidth form b_{pd}. Introducing τB_{if} in this manner assumes that the postdetection filter and integrator operate with perfect efficiency in collecting and integrating all of the statistically independent samples at full amplitude within the total predetection noise bandwidth B_{if}. With this consideration the τB_{if} term carries a practicable prefix, κ, $(\kappa \tau B_{if})$, which for this ideal case is equal to 1. Depending upon the design and efficiency of the postdetection filter, κ will assume lesser values.

Efficient postdetection filtering processes that are accomplished by digital sampling or by true integrating-filters (integrate-and-dump circuits) are examples where $\kappa = 1$. For a single-stage RC filter following the detector $\kappa = (1 - e^{-1})$, and for two cascaded RC filters $\kappa = (1 - e^{-1})^2$. Inefficient postdetection filters have the effect of decreasing the effective integration time with respect to a perfect integrator mainly because the current or voltage waveform at the output of the detector is inefficiently utilized at full amplitude.

The filter term τB_{if} introduced in (2) operates within the idealized constraints that the postdetection bandwidth is small compared to the predetection bandwidth, and that the noise bandwidths of both are equivalently rectangular.

By convention, the radiometric community chooses to use temperature terminology for the specification of radiometer performance rather than power. Conforming with this consideration, (2) can be recast, by the approximation given in Ref. 5 for the equivalence between temperature and power, by substitution of input signal and noise temperatures rather than in power units.

$$\frac{S_o}{N_o} = (\tau B_{if}) \left[\frac{T_{sig}}{(T_{sig} + T_{sys})} \right]^2 = (\tau B_{if}) \left[\frac{T_{sig}^2}{T_{sig}^2 + 2T_{sig}T_{sys} + T_{sys}^2} \right] \tag{3}$$

where T_{sig} and T_{sys} represent the signal and receiver-noise components of the input in kelvins. T_{sys} is explicitly defined, by example, in Fig. 5, as keyed to the functional schematic diagram of the total-power radiometer shown in Fig. 1. It is convenient and conventional to refer T_{sig} and T_{sys} to

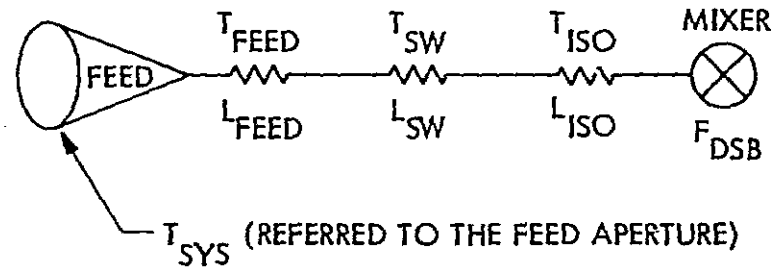

$$T_{SYS} = T_{FEED}\left(L_{FEED}^{-1}\right) + L_{FEED}T_{SW}\left(L_{SW}^{-1}\right) + L_{FEED}L_{SW}T_{ISO}\left(L_{ISO}^{-1}\right) + L_{FEED}L_{SW}L_{ISO}(290)\left(F_{DSB}^{-1}\right), \text{ KELVINS}$$

WHEN: $T_{FEED} = T_{SW} = T_{ISO} = 290$

$$T_{SYS} = 290\left(L_{FEED}L_{SW}L_{ISO}F_{DSB}^{-1}\right), \text{ KELVINS}$$

Fig. 5. System temperature, total-power radiometer

the collecting aperture (or feed) of the total-power receiver rather than to the input of the detector. In doing so, T_{sys} still contains all of the noise contributions from the low-noise IF amplifier, mixer, and RF components - only the reference point has changed. Functionally, the collecting aperture operates as the input port of the total-power radiometer.

The expression for temperature resolution is derived from (3) by the quadratic formula and by letting $S_o/N_o = 1$, with the consideration that $T_{sig} << T_{sys}$, and that τB_{if} is >> 1... a condition normally and easily met in practice.

$$1 = (\tau B_{if}) \frac{T_{sig}^2}{T_{sys}^2} \qquad (4)$$

$$T_{sig}' = \frac{T_{sys}}{\sqrt{\tau B_{if}}}$$

where T_{sig}' is defined as the numerical value of the signal temperature required to produce $S_o/N_o = 1$.

For a host of applications and observations, the assumption that the signal intensity is small compared to the system noise (4) is a good and reliable estimator of the temperature resolution of a total-power radiometer. However, when the signal intensity approaches or exceeds the system noise in (4), it fails as an estimator in a manner of degree because $T_{sig} << T_{sys}$ is violated.

To estimate the degradation in the temperature resolution, as T_{sig} increases with respect to T_{sys}, a Q-factor is derived for the total-power configuration (Q_{tp}) which is to be applied as an operator affecting temperature resolution for the case when $S_o/N_o = 1$, as given in (4). The Q-factor, Q_{tp},

is normalized to the case where $S_o/N_o = 1$ by forming the ratio with the general transfer function form for the detector given by (3). That is,

$$Q_{tp} = \frac{\tau B_{if}\left[\frac{T_{sig}^2}{T_{sys}^2}\right]}{\tau B_{if}\left[\frac{T_{sig}^2}{(T_{sig} + T_{sys})^2}\right]} \qquad (5)$$

$$= 1 + \frac{2T_{sig}}{T_{sys}} + \frac{T_{sig}^2}{T_{sys}^2}$$

Introducing (5) in (4)

$$T'_{sig}\left[T_{sig}, T_{sys}\right]_{tp} = \left[\frac{T_{sys}}{\sqrt{\tau B_{if}}}\right]\left[Q_{tp}\right]$$

$$= \left[\frac{T_{sys}}{\sqrt{\tau B_{if}}}\right]\left[1 + \frac{2T_{sig}}{T_{sys}} + \frac{T_{sig}^2}{T_{sys}^2}\right] \qquad (6)$$

when $T_{sig} \ll T_{sys}$, $Q_{tp} \to 1$.

The cross product term, $2T_{sig}T_{sys}$, which is expressed as a component of the detector-generated noise in (3), emerges as a transformation, $2T_{sig}/T_{sys}$, in the second term of Q_{tp} in (5). For the case where T_{sig} commences to approach T_{sys}, the second and third terms in Q_{tp} rapidly increase and operate to diminish the improvement in T'_{sig} that would otherwise be gained by improving the noise figure or by reducing the RF losses.

Radiometers are frequently operated as comparison devices that compare signal—power variations against a stable noise standard. In the case of the total-power radiometer, the internal noise of the radiometer is amplitude/

stabilized to the greatest possible degree by prudent component selection and circuit design, and is then referred to the feed or collecting aperture by the appropriate thermodynamic temperature transfer equations. At the feed aperture, the referred noise level is used as a stable noise standard against which the signal variations from the signal source are compared directly. Conceptually, the detector is biased by the stable, internally-generated noise level of the RF and IF components and reacts to the component of the total-noise level that fluctuates, i.e., the signal component. When the internal system noise power that is generated within the receiver varies - for any reason - the detector reacts to these noise changes as if they were signal components and the radiometer performance is correspondingly degraded.

Equation (6) is organized as two terms. The first term shows the expected value of the temperature resolution for the case where the signal is small compared to the system noise. In this case the signal-to-noise ratio is set equal to 1. The second term, which is arbitrarily called the Q_{tp} term, is explicitly organized to show the manner in which the temperature resolution varies as a function of the relative magnitudes of the signal and system noise components.

For observations where the signals are small compared to system noise, the first term dominates the consideration for estimating the temperature resolution. This is characteristically the case in many disciplines, such as radio astronomy and microwave spectroscopy. However, for orbital observations of the Earth's surface and its atmosphere, the signal temperatures may commence to become a large fraction of (or even exceed) the system noise, and more rigor is required in the estimation of temperature resolution by invoking the second term which considers the ratios of T_{sig} and T_{sys}.

Frequently it is necessary to perform qualification test measurements on radiometers using blackbody calibration targets whose temperatures are orders of magnitude higher than the actual signal temperatures that will ultimately be observed in field operation. Sometimes it is also expedient and practical to use calibration test targets that are considerably lower than the signal temperatures that will be observed in the practical use of the radiometer. From the foregoing extremes in calibration target temperatures the operational signal temperatures are straddled, in effect, and the signal temperatures that are actually measured can be conveniently and accurately estimated by interpolation. In fact, many radiometer calibration programs attempt to provide calibration temperatures that straddle the expected range of signal temperatures for just this very reason. Always the calibration program should be guided by the expectation that the temperature resolution of the radiometer is functionally related to the calibration target temperatures as they are affected by the ratios of the calibration target temperatures with respect to the system noise, T_{sys}.

The foregoing discussion illustrates the point that a radiometric receiving system is sized in the design stage to operate over a specified range of signal temperatures and to provide a compatible calibration target system. Further, and where practicable, the calibration target temperatures (blackbody radiators or noise sources, for example) are adjusted to include the range of signal temperatures that are expected in the operational use of the radiometer. It is easy to imagine that a bolometer detector system, for example, that was designed for a system noise temperature of several tens of kelvins and for a range of signal temperatures in the order of several millikelvins, would succeed in the measurement of small and subtle temperature gradients on the surface of the sun or the moon.

SIGNAL SUPPRESSION BY DETECTORS

The effect of signal suppression by detectors for small signal-to-noise ratios is easily observable in the laboratory by the equipment illustrated in Fig. 6, and as described in Ref. 7. An IF amplifier, with detector and filter attached, serves to simulate the receiver components under consideration. The IF amplifier has low gain and a wide dynamic range so that overload is never approached or considered. A CW carrier f_o is generated by the signal generator and modulated to produce modulation products, one of which is $(f_o - f_m)$, where f_m is an audio-modulation frequency. A broadband noise source is introduced into the input of the IF amplifier along with the modulation products from the signal generator. At the output of the detector filter, a narrow bandpass-filter is selectively tuned to $(f_o - f_m)$. An arbitrary gain setting of the IF amplifier sets a nominal noise level at the input to the detector where the noise is generated by the first stage of the IF amplifier. The intensity of $(f_o - f_m)$ is adjusted at the signal generator to produce a full-scale reading on M2 with the attenuator at the output of the broadband IF noise generator set to a very large value of attenuation. When the attenuator is reduced to <u>increase</u> the noise level in the predetection bandwidth, the meter reading on M2 <u>decreases</u>. That is, as M1 increases M2 decreases. The fact that M2 decreases is contrary to the expected result when noise and signals are mixed in additive power relationships. Actually, the destruction (suppression) of the signal component within the bandpass filter is manifested by the decrease in signal level on M2 when the predetection noise level is increased. In fact, the reduction in M2 occurs at a greater rate than a uniform increase in M1. The harmonics and cross products produced in the detector, at the expense of signal energy, account for its suppression. That is, the S × S,

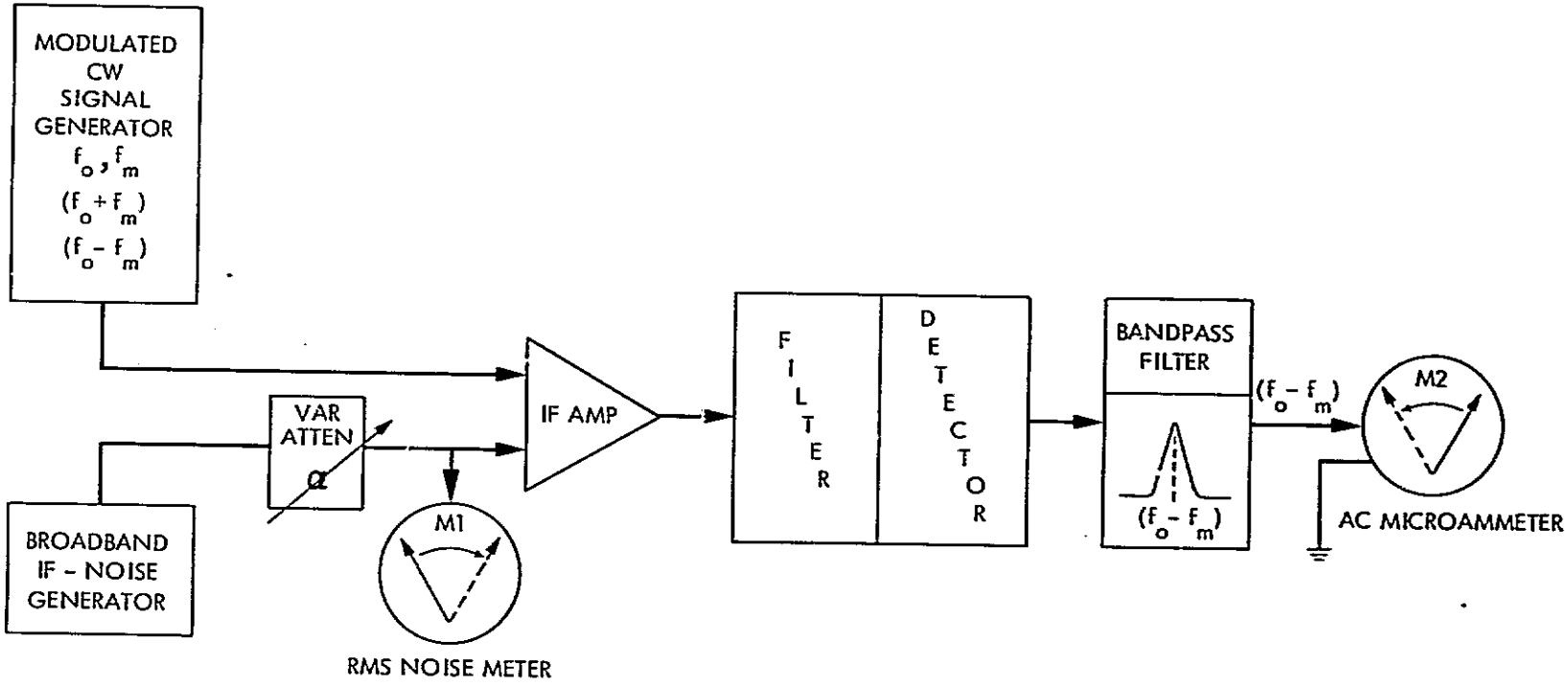

Fig. 6. Signal suppression by detectors

S × N, and N × N components operate to redistribute the signal energy elsewhere in the bandpass, where they become indistinguishable from receiver noise. The example given here employs a sideband of a modulated CW signal generator to produce a test signal. This method is adopted for simplicity to illustrate the concept of signal suppression but the expected result would be significantly similar if the circuitry were configured to respond to a noise signal.

THE TRANSFER FUNCTION AND THE SENSITIVITY OF THE MODULATED RADIOMETER

The input-output relationships for the modulated radiometer appear in many forms and are treated abundantly in various levels of detail in the technical literature. The responses of the modulated radiometer and its sensitivity are importantly affected by the character of the switching waveform. From Fig. 1, it is seen that the switching waveform synchronizes the RF modulator switch and the synchronous detector or correlator at the output. In all cases, a square-wave switching waveform, for both the RF modulator switch and the signal correlator (synchronous detector), produces the most optimal results. In many cases the electrical or mechanical peculiarities of the modulator switch itself importantly affect the exact shape of the switching waveform. For example, chopper wheels, mechanical waveguide or coaxial switches, and certain categories of magnetic materials which are used as RF switches produce rather complex waveforms that are intrinsic to their own internal operation and are somewhat independent of the driving function which may be a sinusoidal or a square waveform. Sinusoidal modulation waveforms for both the RF modulator and the correlator are convenient to use because the waveform is easily generated. When the ultimate in sensitivity is needed, however, the square-wave modulation is applied to both the RF modulator and the correlator. The most common

combinations of RF modulator and correlator waveforms are: (1) sinusoidal RF modulation with sinusoidal correlation; (2) square-wave RF modulation with sinusoidal correlation; and (3) square-wave RF modulation with square-wave correlation. Sometimes modulation waveforms are adopted to be compatible with what is available or possible in a given system design, and space, weight, or cost limitations can prevent the inclusion of elaborate waveform-shaping features.

The shape of the waveform that synchronizes the correlator is also important because it affects the operation of the detector and its output products. Actually, the terms of the transfer function, as will be seen later, are impacted by the waveforms that drive both the modulator and the correlator. Again, the assumption prevails that the detector is the only nonlinear device in the modulated radiometer over its total dynamic range of signal temperatures. The modulation waveform and its harmonic products interact with the detector and modify its rectification properties and its output waveform. These can usually be expressed at the input of the detector by the Fourier coefficients of the modulation waveform in the case of square-wave modulation or by the amplitude envelope of the sinusoidal waveform.

S. J. Goldstein, Jr. has developed the transfer function of the modulated radiometer as affected by the modulation waveform and as influenced by the square-law detector (Ref. 8). In turn, W. A. Johnson has introduced some corrections and has concisely stated the transfer functions for several combinations of RF modulator and correlator waveforms (Ref. 9). Notably, D. F. Wait (Ref. 12) further identifies a correction to the coefficient for the cross product term for the square-wave modulation and square-wave correlation

expression given by Johnson (Ref. 9). The expressions developed by Goldstein and Johnson (Refs. 8, 9) are important because they explicitly show the influence of the detector and the modulation waveforms on the transfer functions, and how the temperature resolution is affected.

The statistical forms given for the transfer functions (Refs. 8, 9) are recast and adapted here in (7) to illustrate the similarity between the total-power and modulated radiometer transfer functions as they are influenced by the detector and the modulator waveform. The mathematical forms are basically the same except that the transfer function for the modulated radiometer contains coefficients for the terms that are influenced by the modulation waveform for the RF switch and the synchronous detector. The coefficients shown in (7) are given for the case where both the modulator switch and the synchronous detector are driven by a square wave and where the relative phase adjustment between the switch and detector are optimized. The coefficients for other combinations of modulation waveforms are given by Goldstein and Johnson (Refs. 8, 9).

$$\frac{S_o}{N_o} = \left[\frac{\tau B_{if}}{4}\right]\left[\frac{P_i^2}{\left(\frac{P_i^2}{2} + P_i N_i + N_i^2\right)}\right] \tag{7}$$

or, by temperature equivalence

$$\frac{S_o}{N_o} = \left[\frac{\tau B_{if}}{4}\right]\left[\frac{T_{sig}^2}{\left(\frac{T_{sig}^2}{2} + T_{sig}T_{sys} + T_{sys}^2\right)}\right] \tag{8}$$

where, for the modulated radiometer case, T_{sig} and T_{sys} are referred to the input port of the modulator switch.

Apparently, (7) and (8) have the same functional form as given for the total-power radiometer in (2) and (3).

When $T_{sig} << T_{sys}$ and where S_o/N_o is set equal to 1 then (8) reduces to

$$\frac{S_o}{N_o} = \left[\frac{\tau B_{if}}{4}\right]\left[\frac{T_{sig}^2}{T_{sys}^2}\right]$$

$$1 = \left[\frac{\tau B_{if}}{4}\right]\left[\frac{T_{sig}^2}{T_{sys}^2}\right] \tag{9}$$

$$T'_{sig} = \frac{2T_{sys}}{\sqrt{\tau B_{if}}} \tag{10}$$

The temperature resolution of the modulated radiometer is a function of the signal temperature, and to estimate the degradation in the temperature resolution as T_{sig} increases with respect to T_{sys}, a factor Q_m is calculated that may be applied as an operator on the temperature resolution when the signal-to-noise ratio equals unity.

$$Q_m = \frac{\left[\frac{\tau B_{if}}{4}\right]\left[\frac{T_{sig}^2}{T_{sys}^2}\right]}{\left[\frac{\tau B_{if}}{4}\right]\left[\frac{T_{sig}^2}{\frac{T_{sig}^2}{2} + T_{sig}T_{sys} + T_{sys}^2}\right]} \tag{11}$$

$$Q_m = 1 + \frac{T_{sig}}{T_{sys}} + \frac{T_{sig}^2}{2\,T_{sys}^2} \tag{12}$$

Rewriting (10) with (12), the temperature resolution for the square-wave modulated and square-wave demodulated radiometer is expressed by

$$T'_{sig}\,(T_{sig},\, T_{sys}) = \left[\frac{2\,T_{sys}}{\sqrt{\tau B}}\right]\left[Q_m\right] = \left[\frac{2\,T_{sys}}{\sqrt{\tau B}}\right]\left[1 + \frac{T_{sig}}{T_{sys}} + \frac{T^2_{sig}}{2T^2_{sys}}\right] \tag{13}$$

In practical measurements of T'_{sig}, the accuracy of the estimate given by (13) is strongly influenced by the accuracy of the numerical values that are entered for T_{sig}, T_{sys}, τ, and B_{if}. In general, unless clinical attention to detail is exercised, large errors in these input quantities can occur.

T_{sig}, for example, is the signal temperature appearing at the input port of the modulator switch; it contains both signal-temperature contributions from the target and the emission temperature from the transmission components that interconnect the antenna and the input port of the modulator switch.

Dissipative losses in RF components must be accurately accounted for in calculating T_{sig}. Typically, dissipative loss measurements of radiometer components tend to be based on the best values measured under laboratory conditions, and the losses of components surviving quasiproduction tests and quantities are higher. This is especially true of noise-figure measurements. Moreover, noise-figure measurements must finally be referenced to a 290 K reference temperature when submitted as a measured value--frequently, and unfortunately, this requirement is ignored, neglected, or waived. Also, noise figures are vulnerable to aging and physical temperature variations. Reactive losses (VSWR) occurring between RF components are difficult to account for and

are frequently neglected. Individual component measurements, in general, require meticulous measurement precision on an individual basis; otherwise, the accumulated losses can become a significant fraction of the total loss measurement for all the components--especially when the total losses are small.

The accuracy of the temperature resolution estimate given in (13) is also importantly affected by the character and purity of the waveform for the modulator switch and the synchronous detector. RF switches, for example, may be driven optimally by a square waveform but the modulated noise waveform emerging from the switch frequently appears as a relatively complex waveform--sometimes even triangular or near-sinusoidal. The same comments similarly apply to the effective output waveform of the synchronous detector. The synchronous detector is critically responsive to the phasing adjustments between its comparative output circuits. Phase adjustments may change with temperature or time, or may not have been set correctly initially.

The first term in (13) estimates the temperature resolution for the case where the signal-to-noise ratio equals unity. Basic assumptions are made that affect the accuracy of the estimate of the temperature resolution with this term that should be honored in the practical design of the radiometer circuits. Predetection/postdetection bandwidth ratios, filter designs, integrator efficiencies, and time constants should be consistent with the basic assumptions.

In the practical design of radiometer systems, however, many technical compromises are made to reconcile the continual conflicts among performance excellence, time schedules, and costs, and to this extent performance invariably suffers to a degree.

As with the total-power radiometer the effect of the postdetection filter that follows the detector emerges as a consideration. In the functional forms,

are frequently neglected. Individual component measurements, in general, require meticulous measurement precision on an individual basis; otherwise, the accumulated losses can become a significant fraction of the total loss measurement for all the components--especially when the total losses are small.

The accuracy of the temperature resolution estimate given in (13) is also importantly affected by the character and purity of the waveform for the modulator switch and the synchronous detector. RF switches, for example, may be driven optimally by a square waveform but the modulated noise waveform emerging from the switch frequently appears as a relatively complex waveform--sometimes even triangular or near-sinusoidal. The same comments similarly apply to the effective output waveform of the synchronous detector. The synchronous detector is critically responsive to the phasing adjustments between its comparative output circuits. Phase adjustments may change with temperature or time, or may not have been set correctly initially.

The first term in (13) estimates the temperature resolution for the case where the signal-to-noise ratio equals unity. Basic assumptions are made that affect the accuracy of the estimate of the temperature resolution with this term that should be honored in the practical design of the radiometer circuits. Predetection/postdetection bandwidth ratios, filter designs, integrator efficiencies, and time constants should be consistent with the basic assumptions.

In the practical design of radiometer systems, however, many technical compromises are made to reconcile the continual conflicts among performance excellence, time schedules, and costs, and to this extent performance invariably suffers to a degree.

As with the total-power radiometer the effect of the postdetection filter that follows the detector emerges as a consideration. In the functional forms,

given here, both the predetection and postdetection noise bandwidths are equivalently rectangular, with the further assumption that the postdetection bandwidth is much smaller. If an efficient waveform sampling device operates directly on the output of the detector--such as an integrating sample-and-hold circuit cooperating with a computer, or an efficient waveform integrator such as an integrate-and-dump circuit--then an efficiency factor κ, applied directly to (τB_{if}) under the radical in (13), is equal to 1. Any inefficiencies in the filter that follows the detector operate to reduce the effective integrated area within the postdetection noise bandpass and reduce the time constant. For a single RC circuit following the detector $\kappa = (1 - e^{-1})$.

THE INPUT CIRCUIT OF THE MODULATED RADIOMETER

The true input terminal of the modulated radiometer is the signal port of the modulator switch. This is true because the modulator switch synchronizes the modulation of the signal energy that is recognized and demodulated by the synchronous detector. Further, it is assumed that all internal losses within the modulator switch are symmetrical. By design, the system noise generated by the mixer and internal amplifier components are referred forward to the input port of the modulator switch and remain unmodulated. The information appearing at the input port of the modulator switch contains both the emission temperatures from the lossy components intervening between the feed aperture and the signal temperatures viewed by the feed aperture. Conceptually, external target temperatures are reduced by the dissipative losses in the components and finally appear at the signal input port of the modulator switch as signal temperature fluctuations riding on a temperature pedestal produced by the emission

from the transmission and calibration components. When the component losses are high and the target temperatures are low, the actual target temperatures may appear as a relatively small percentage of T_{sig}. The temperature pedestal is modulated identically with the target temperature component, and the synchronous detector cannot distinguish between a bona fide change in the target temperature or a change in the emission temperature of the input circuit losses. For this reason, the thermal stabilities and circuit variations of the input transmission and calibration components importantly affect the output-signal response of the microwave radiometer. In fact, more than one radiometer system has failed because of inadequate attention to detail in the design of the input transmission and calibration circuits.

The basic equations that effect the thermodynamic transfer of energy through the transmission circuits to the input port of the radiometer are shown in Figs. 7 and 8. The blackbody target temperature is transferred through the waveguide and switch losses to the input of the modulator switch, T_{sig}. The losses, which are identified by L_o for the feed, are principally caused by the orthomode transducer and waveguide-matching sections. L_g symbolizes the waveguide loss, and L_s and L_c signify the dissipative losses attributable to calibration switches (see Fig. 1). The dissipative losses are expressed as dimensionless quantities greater than 1. All reactive losses are assumed to be insignificant. The physical temperatures of the lossy components, which are symbolized by a capital T, are subscripted to agree with the associated dissipative losses. An inspection of the respective terms in the thermodynamic transfer equation clearly identifies the many elements of the transmission network that can affect the value of T_{sig} that are not represented by bona fide target-temperature changes.

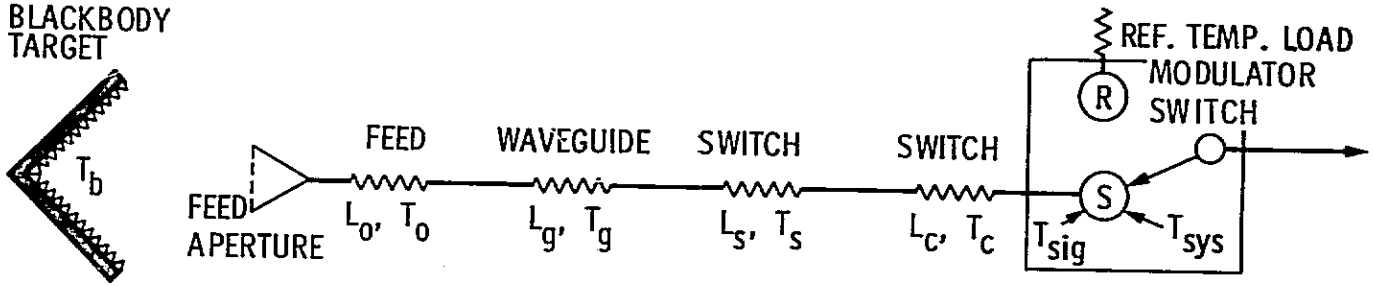

$$\frac{T_b}{L_o L_g L_s L_c} + \frac{T_o (L_o - 1)}{L_o L_g L_s L_c} + \frac{T_g (L_g - 1)}{L_g L_s L_c} + \frac{T_s (L_s - 1)}{L_s L_c} + \frac{T_c (L_c - 1)}{L_c} = T_{sig}$$

WHEN: $T_b = T_o = T_g = T_s = T_c$

$T_b = T_{sig}$ (INDEPENDENT OF DISSIPATIVE LOSSES)

Fig. 7. Modulated radiometer (thermodynamic transfer of energy), signal temperature T_{sig}

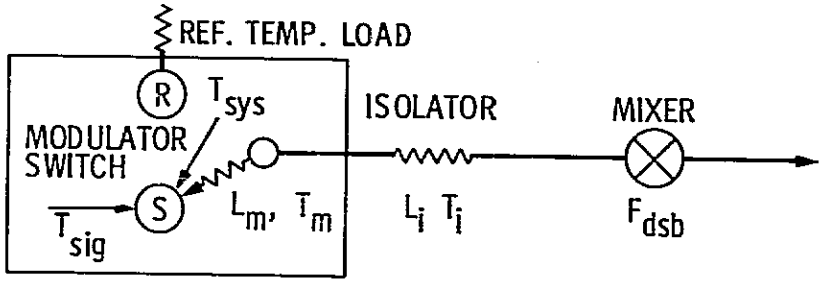

$$T_{sys,} = T_m (L_m - 1) + L_m T_i (L_i - 1) + L_m L_i (290) (F_{dsb} - 1)$$

WHEN: $T_m = T_i = 290$

$T_{sys} = 290 (L_m L_i F_{dsb} - 1)$, KELVINS

Fig. 8. Modulated radiometer (thermodynamic transfer of energy), system temperature T_{sys}

Given also in Fig. 5 is the expression for referring the system temperature to the input port of the modulator switch. In this example, the double-sided noise figure is used with the inference that a superheterodyne receiver is employed (Ref. 13). Fig. 9 illustrates an example of the bandpass responses of a typical radiometer where the double-sided noise figure is justified. Notably, the system noise temperature, T_{sys}, is constant and unmodulated. At this point one can readily identify the elements that comprise T_{sig} and T_{sys} as they appear in the basic transfer functions (7) and in the expression for temperature resolution (13). The ratios of these temperatures importantly affect the linearity of the radiometer response, under certain conditions, as expressed by the output signal-to-noise ratios given in (7).

The component of T_{sig} represented by the dissipative losses, i.e., the noise pedestal, is sometimes large and is subject to thermal instabilities and mismatch losses that may be large compared to the component of the blackbody target temperatures arriving at the input port of the modulator switch. Fig. 10 elucidates the point by example. The thermodynamic temperature transfer equations are reproduced with dissipative loss examples given. It is assumed that the lossy components are all at the same physical temperature, i.e., 300 K. Some useful input circuit considerations are expressed in the example. When the target temperature and the temperature of the losses are identical, T_{sig} remains at the target temperature <u>irrespective of the loss variations</u>. Also, from the same temperature relationships it is seen that even when the target temperature fictitiously approaches zero kelvins, T_{sig}, because of the emission pedestal, approaches 59 K. For blackbody target temperatures less than 300 K, T_{sig} is greater than the target temperature. When the blackbody target temperatures exceed 300 K, T_{sig} is less than the target temperature. Then,

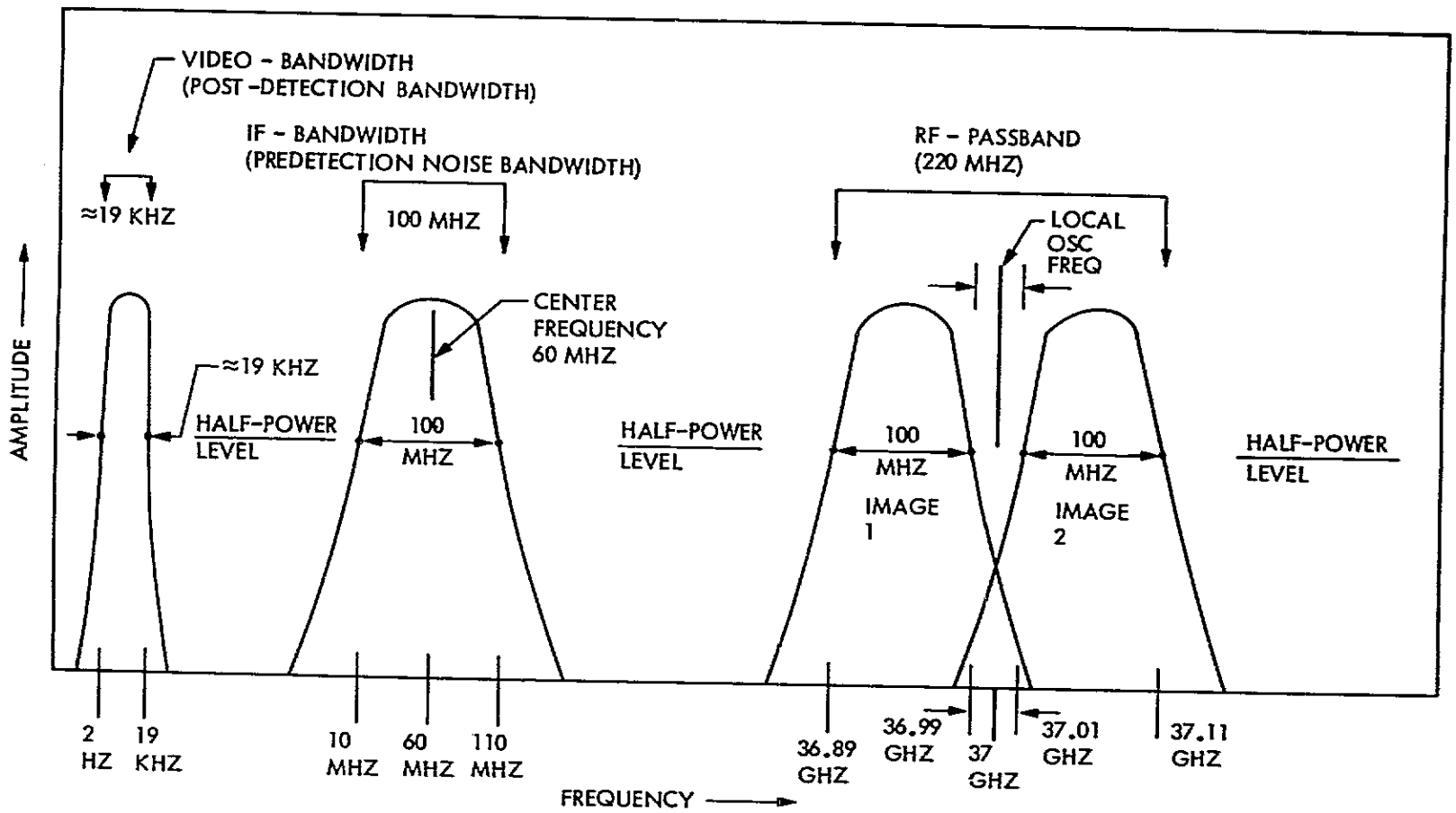

Fig. 9. Superheterodyne radiometer responses (example at 37 GHz center frequency)

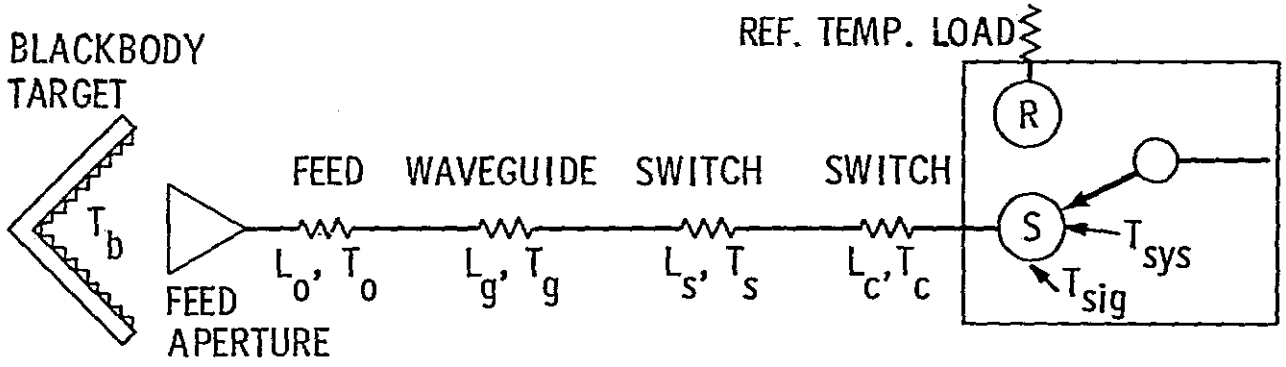

$$\frac{T_b}{L_o L_g L_s L_c} + \frac{T_o(L_o - 1)}{L_o L_g L_s L_c} + \frac{T_g(L_g - 1)}{L_g L_s L_c} + \frac{T_s(L_s - 1)}{L_s L_c} + \frac{T_c(L_c - 1)}{L_c} = T_{sig}$$

DISSIPATIVE LOSSES ASSUMED FOR THE EXAMPLE

$L_o = 0.3$ dB

$L_g = 0.2$ dB

$L_s = 0.23$ dB

$L_c = 0.23$ dB

AND THE THERMOMETRIC TEMPERATURE OF THE LOSSES:

$T_o = T_g = T_s = T_c = 300$ K

WHEN THE TEMPERATURES OF ALL THE LOSSES ARE 300 K, THEN

$T_{sig} = T_b/(L_o L_g L_s L_c) + 59.49$ K

	BRIGHTNESS TEMP. OF SIGNAL AT THE FEED APERTURE, T_b, KELVINS	EMISSION TEMPERATURE OF SIGNAL AND RF LOSSES AT THE ISOLATOR SWITCH PORT, T_{sig}, KELVINS
	.00	59.49
	1.00	60.29
	2.00	61.09
COSMIC BACKGROUND	2.70	61.66
	3.00	61.90
	4.00	62.70
LIQUID HELIUM	4.20	62.86
	5.00	63.50
	6.00	64.30
	7.00	65.10
	8.00	65.91
	9.00	66.71
	10.00	67.51
	20.00	75.53
LIQUID HYDROGEN	20.46	75.85
	30.00	83.54
	40.00	91.56
	50.00	99.58
	60.00	107.59
	70.00	115.61
	77.00	121.22
LIQUID NITROGEN	77.36	121.51
	78.00	122.02
	80.00	123.63
	87.00	129.24
LIQUID ARGON	87.30	129.48
	88.00	130.04
	90.00	131.64
LIQUID OXYGEN	90.20	131.80
	100.00	139.66
	110.00	147.68
SOLID METHANE	111.70	155.69
	120.00	155.69
	130.00	163.71
	140.00	171.73
	150.00	179.74
	160.00	187.76
	170.00	195.78
	180.00	203.79
	190.00	211.81
SOLID CARBON DIOXIDE	194.50	215.42
	195.00	215.82
	200.00	219.83
	210.00	227.84
	220.00	235.86
	230.00	243.88
	240.00	251.89
	250.00	259.91
	260.00	267.93
	270.00	275.94
ICE	273.16	278.48
	280.00	283.96
	290.00	291.98
	300.00	300.00
	310.00	308.01
	320.00	316.03
	330.00	324.05
	340.00	332.06
	350.00	340.08
	360.00	348.10
	370.00	356.11
BOILING WATER	373.16	358.65
	380.00	364.13
	390.00	372.15
	400.00	380.16

Fig. 10. Thermodynamic temperature transfer

apparently, the physical temperature of the lossy components sets the relative-temperature transition point for the target-T_{sig} relationship.

Accountability for, and the prudent and meticulous design of, the transmission circuits between the cold calibration target (e.g., a sky horn as shown in Fig. 1) and the input port of the modulator switch are of critical importance, because, in this common case, the emission temperatures of the passive intervening components which are superposed upon the cosmic background temperature combine to form the actual cold calibration temperature (Ref. 14). The thermodynamic transfer equations and the worked example given for a specified set of circuit losses amply illustrate the point in Fig. 10. When the accumulated RF circuit losses in the cold calibration circuit are 0.96 dB, for example, the emission temperature viewed by the input port of the modulator switch is 62 K when viewing the cosmic background. The cold calibration temperature is dominated by the emission from the RF loss elements, and the actual sky contribution is very small.

The blackbody target is a key component in the qualification of the performance of a radiometer system. Measurements of subtle input-output relationships and the calibration of a radiometer rigorously depend upon the availability of reliable blackbody targets.

The thermodynamic temperature relationships given in Fig. 10 consider only the dissipative losses of the components involved. In addition to the dissipative losses, there are reactive losses arising from impedance mismatches among the individual components and in the junctions between components. The reactive losses are observed as voltage standing wave ratios (VSWR's), and patently operate to introduce losses which affect the noise level of the RF transmission system. Prudence in the design of the RF section of a radiometer suggests that

considerable effort should be expended to maintain the reactive losses to a degree where they are insignificant with respect to the dissipative losses. Otherwise, precise accountability for the effects of reactive junctions requires accurate measurements of both phase and amplitude of all the participating RF components both individually and in combination in the final operating configuration. Moreover, for high accuracy, the variations in the VSWR with respect to physical temperature changes among the component junctions must be individually confirmed by measurement.

OPERATIONAL INSIGHT OF A MODULATED RADIOMETER

A discussion of the detailed operating principles and circuits of a modulated radiometer is useful and informative. The discussion objectives are best served by example where typical numerical values are adopted for key circuits and components and where target and reference temperatures are identified and traced from the antenna to the digital output, where they appear as the usable signal responses that are available for immediate use or for archive.

The example is keyed to the circuit configuration for a modulated radiometer as shown in Fig. 2, where the RF components, losses, and physical temperatures are mathematically symbolized and shown schematically in Fig. 11.

The mathematical quantities are defined as the model develops with the commentary that the decibel quantities given for the various RF component losses are expressed in exponential form (i.e., $10^{dB/10}$) and thus enter the terms of the equations as dimensionless numbers greater than one.

Numerical values are assigned to the respective loss elements with the intent to reflect performance values that are sometimes encountered in practice.

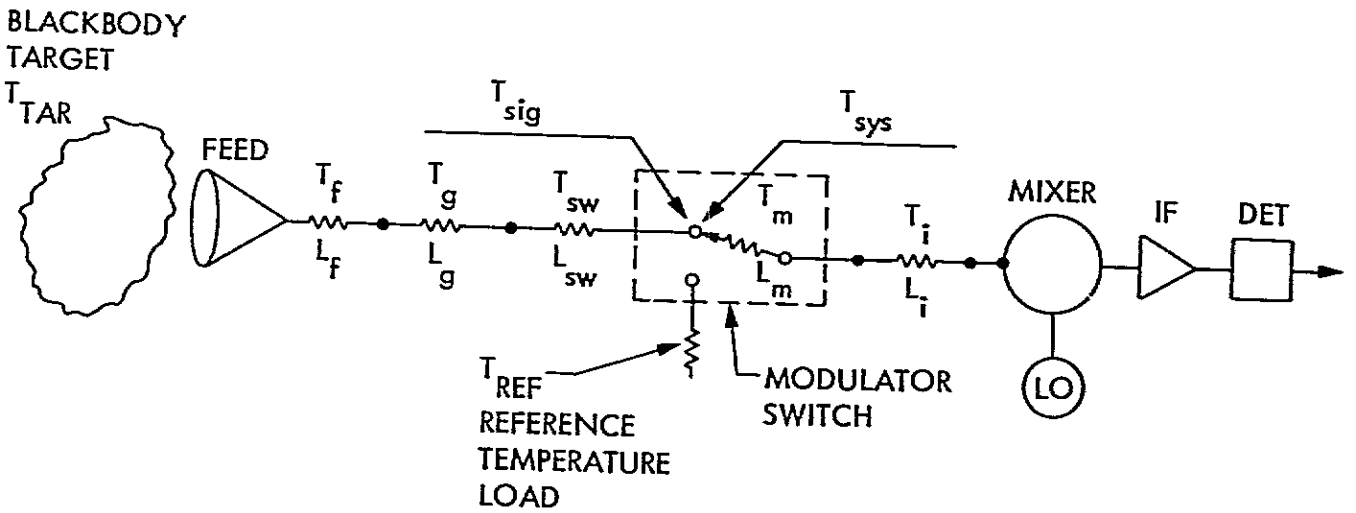

Fig. 11. Functional-model schematic diagram

Occasionally, it may be useful to refer to previous expressions developed or defined in this monograph in order to review the motivation for the structure of the mathematical forms.

In proceeding with the development of the radiometer model, by example, one is counselled to be continually aware of the distinction between thermometric and thermodynamic temperatures. In particular, thermodynamic temperatures are transferred on an instantaneous basis and are generally considered to be the Planckian-approximation equivalent (Ref. 5) for the transference of power. Platinum and mercury thermometers measure thermometric temperatures.

A clear distinction is needed concerning the terminology relating to detector components. The mixer, for example, is functionally a frequency converter that usually translates RF energy at microwaves to lower frequencies. Under typical operating conditions, the mixer is "biased" by a local CW-oscillator whose input power level into the mixer assembly ranges in the order of several milliwatts, and is expected to be many orders of magnitude greater than any anticipated input signal; viz., signal intensities range from picowatts to microwatts. When the mixer is operated with a large ratio of power levels between the signal and local oscillator, the output power at IF frequencies is expected to be linearly proportional to the input signal power and to conform to the classical mixer conversion equation $P_o = k\ E_i^2$, where P_o is the output power from the mixer, k is a conversion efficiency constant, and E_i is the RMS value of the input voltage waveform.

Here an important distinction is made in the relationship between the bias levels and signal levels for the mixer and ν-th law detector. The ν-th law detector is biased by the internal receiver noise, T_{sys}, which is unmodulated

noise possessing stationary statistics and whose thermodynamic temperature is referenced forward from the mixer/IF unit to the input port of the modulator switch.

At the input to the ν-th law detector the modulated noise-signal waveform arrives within the same noise-bandwidth (predetection IF bandwidth) as the system-noise bias. Here the significant difference between the signal and bias power levels for the mixer and the ν-th law detector is dramatically visualized; that is, the modulated signal waveform power level entering the mixer is, by design and by expectation, always orders of magnitude smaller than the local CW-oscillator bias power level. Per contra, at the input to the ν-th law detector the modulated signal may range from a small fraction of the stationary system-noise bias level, to where it approaches or, indeed, may even exceed the noise bias level. When the latter condition prevails, in a matter of degree, the assumption fails that the output power from the ν-th law detector is linearly proportional to the input signal power, and the behavior of the ν-th law detector is better explained by its general signal-to-noise transfer properties than by the special case where $P_o = k E_i^2$, which patently fails.

The circumstances that produce the condition where the power in the signal waveform approaches or exceeds the power level of the system-noise bias are exemplified in a remote-sensing application where the system-noise temperature is driven to very low values to achieve good temperature resolution, but at the same time is required to observe targets whose signal temperatures vary over a wide dynamic range. Consider the instance where the system temperature has been reduced to a 100 K level by a cryogen-cooled mixer or detector, and the observing sequence requires alternate observations of the sky background at 2.7 K and of the earth at 290 K. A similar situation occurs in an astronomical

observing situation where it is desired to observe millikelvin temperature variations on the moon's surface (on a mean surface temperature of 240 K) with a 25-K noise-temperature device that depends on alternate observations of the sky background for a cold calibration. The foregoing are offered as examples where the range of signal temperatures may strongly impact the expected performance of the radiometer because of the relative power levels of the bias and signal waveforms at the ν-th law detector. It is necessary to further recognize that these relationships are intrinsic to the operation of the ν-th law detector itself and to presume that associated circuits are not so amplitude-stressed or overloaded as to obscure the reactions of the ν-th law detector with the signal and bias waveforms.

The ν-th law detector is inextricably locked with the circuits that precede and follow it. In this context the IF amplifier chain serves as the predetection bandwidth determinant for the modulated signal components and as the noise bandwidth for the system noise. Notably, the IF amplifiers identically operate on both the signal and system noise waveforms in the sense that gain variations similarly affect both. Conceptually, the signal and bias waveforms are introduced into the ν-th law detector by a single port as is sometimes done with the signal and local oscillator waveforms as they are introduced into a mixer assembly. The bandwidth of the video amplifier, following the ν-th law detector, is frequently designed to pass the higher order harmonics of the squarewave switching waveform - commonly to the 10th harmonic and greater.

To complete the discussion of detector terminology, attention is directed to the synchronous detector that follows the ν-th law detector and video amplifier. The synchronous detector operates mainly as a relative-amplitude signal-comparator and does not function as a detector in the general sense of the word. Functionally, the synchronous detector compares the detected wave-

form arriving from the ν-th law detector when it alternately observes the signal and reference-temperature load. In this comparison mode, incidental gain variations in the mixer and amplifier chain are, importantly, suppressed in a subtractive process. The synchronous detector and the modulator switch-rate are presumed to be synchronized by a large-amplitude square-wave where careful circuit design considerations maintain extremely small time displacements between the switching of the modulator switch and the synchronization of the synchronous detector. Normally, with good circuit-design practice, the synchronous detector does not affect the sensitivity or dynamic signal range of the radiometer.

Returning to the discussion of the front-end operation of the radiometer, and again, by example, with reference to Fig. 11 some very important, and often overlooked, properties of the RF transmission circuits as they affect T_{sys} and T_{sig} are discussed.

Dissipative losses for the RF components are adopted to implement the discussion as follows:

L_f = Feed losses (0.1 dB)

L_{wg} = Waveguide losses (0.2 dB)

L_{sw} = Switch losses in the signal position (0.3 dB)

and with the further understanding that reactive losses, produced by voltage standing wave ratios, are consistently negligible.

Now

- T_m and L_m symbolize the physical temperature and dissipative loss for the modulator switch.
- T_i and L_i symbolize the physical temperature and the dissipative loss for the isolator.

When

$$T_m = T_i = 300 \text{ K}$$

and

$$L_m = 0.25 \text{ dB}$$

$$L_i = 0.15 \text{ dB}$$

$$F_{dsb} = 3.5 \text{ dB}$$

then referring to Fig. 8, T_{sys} is calculated first from these assumptions:

$$T_{sys} = 300\,(10^{0.25/10} - 1) + 10^{0.25/10}(300)(10^{0.15/10} - 1) + 10^{0.25/10}10^{0.15/10}(290)(10^{3.5/10} - 1)$$

$$= 17.776 + 11.167 + 393.887$$

$$= 422.83 \text{ K}$$

Now the thermometric temperatures of the dissipative components in the RF signal transmission line in Fig. 11 are defined to be

$$T_f = T_g = T_{sw} = 300 \text{ K}$$

T_{tar} is defined to be a blackbody target with an emissivity equal to one, whose thermometric temperature is 300 K.

With these baseline assumptions for the thermometric temperatures of the lossy components in the signal transmission line and the blackbody target, it is seen that the target temperature T_{tar}, as referred to the input port of the modulator switch, is maintained at 300 K regardless of the numerical value of any of the component losses (see Fig. 7). Because of this unique condition relating the target temperature, RF component losses, and the temperature of the target referred to the input port of the modulator switch (the receiver input port), this circuit condition is useful and is commonly adopted as a reference test condition for basing many radiometer performance tests.

For this example, T_{tar} is transformed by the thermodynamic transfer of energy to T_{sig} by

$$T_{sig} = \frac{T_{tar}}{L_f L_{wg} L_{sw}} + \frac{T_f(L_f - 1)}{L_f L_{wg} L_{sw}} + \frac{T_{wg}(L_{wg} - 1)}{L_{wg} L_{sw}} + \frac{T_{sw}(L_{sw} - 1)}{L_{sw}} \quad , K$$

$$= \frac{300}{10^{0.1/10}\,10^{0.2/10}\,10^{0.3/10}} + \frac{300\,(10^{0.1/10} - 1)}{10^{0.1/10}\,10^{0.2/10}\,10^{0.3/10}}$$

$$+ \frac{300\,(10^{0.2/10} - 1)}{10^{0.2/10}\,10^{0.3/10}} + \frac{300\,(10^{0.3/10} - 1)}{10^{0.3/10}}$$

$$= 261.29 + 6.086 + 12.601 + 20.024$$

$$= 261.29 + 38.711 \text{ K}$$

$$= 300.0 \text{ K}$$

In the practical operation of the radiometer it is convenient to consider that the target temperature variations are viewed from the input port of the radiometer, which is here defined as the signal port of the modulator switch. In this sense, then, variations in target temperatures, as they arrive at the modulator switch, are modified by the signal transmission components intervening between the antenna and the signal port of the modulator switch. That is, when the antenna views a target temperature change from 300 to 2.7 K, the signal port of the modulator switch sees a considerably smaller change as influenced by the losses in the transmission line components. Referring to the modeled example shown in Fig. 11, for a target temperature change from 300 to 2.7 K, the signal port of the modulator switch observes a change from 300 K to a minimum temperature of $2.7/(L_f L_g L_{sw})$ + 38.711 K or 41.06 K. In this example, then, the output response of the radiometer, i.e., the relative digital numbers, will report a temperature change of only 258.94 K whereas the actual target temperature change was actually 300 - 2.7 = 297.3 K. Consider-

ation of these input-temperature changes and output-response relationships are of enormous importance when calibrating a radiometer system and calculating the temperature resolution and the gain scale factors.

In these analyses the target component of the signal, the emission pedestal produced by the dissipative losses in the signal line, and the system noise temperature are separately identified, and reckoned with, until they arrive at the input of the ν-th law detector.

It is relevant and useful to restate:

(1) target temperature variations

(2) emission-pedestal temperature variations in the signal line

(3) system noise

(4) emission from the reference-temperature-load

all converge at the input-port of the radiometer and can be separately identified and quantified.

Gain variations occurring in the mixer and amplifier chain, following the input port of the modulator switch, similarly--if not identically--affect all at any instant of time.

At this juncture, it will be useful to discuss the circuit elements of the radiometer, following the ν-th law detector, that deal with the detected signal waveforms. This material will functionally serve to preface a series of computations that illustrate the expected output signal-to-noise ratios given by several target temperatures.

A functional block diagram of the circuits following the ν-th law detector is given in Fig. 12. Immediately following the detector and video amplifier is the synchronous detector or correlator, which compares the signal (SIG) and reference-temperature-load (RTL) waveforms in a subtractor circuit element

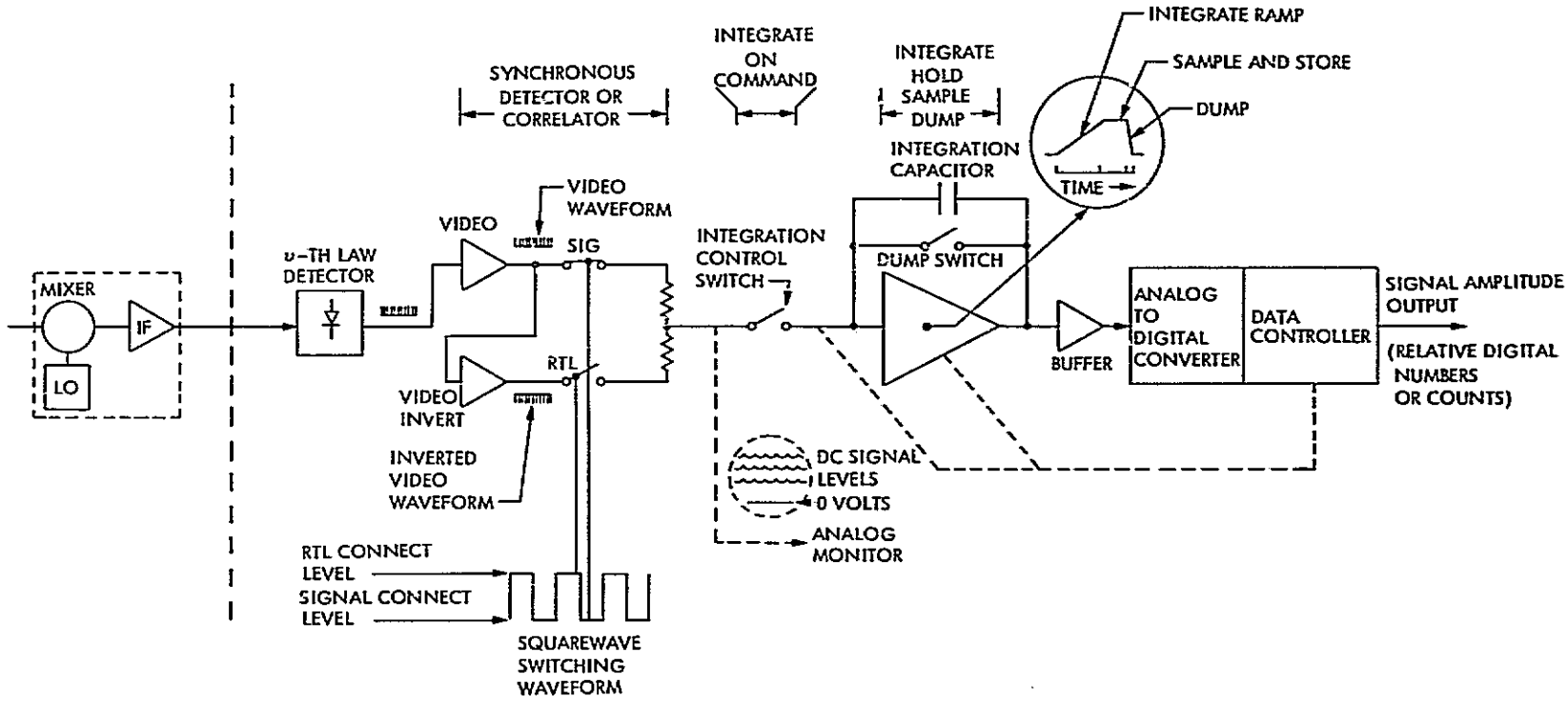

SWITCH STATUS

SIG CLOSED WHEN SIGNAL-PORT OF MODULATOR SWITCH IS CONNECTED TO MIXER

RTL CLOSED WHEN REFERENCE-TEMPERATURE-LOAD PORT OF MODULATOR SWITCH IS CONNECTED TO MIXER

Fig. 12. Functional operation synchronous correlator (detector)

as shown schematically by a center-tapped resistor. As shown symbolically by the DC signal levels emerging from the synchronous detector, the output signal levels are offset to produce a range of DC voltages that are positive in sign and offset from zero volts by an arbitrary amount. That is, when target temperatures range from say 50 to 300 K, the DC offset produces a range of corresponding positive voltages. Many convenient output signal arrangements are possible here by organizing the interaction between the squarewave switching waveform and by adjusting the temperature of the reference temperature load. In principle, and sometimes in practice, the DC signals may respond to the target temperature variations by moving in both positive and negative directions about zero, or by ordering larger and larger negative voltage swings with increasing target temperatures.

Following the synchronous detector components is the integration circuitry. In this segment of the radiometer the integration-control-switch, the dump switch, and the sample-and-hold circuits are under the continual control of the data controller unit. Timing is ordered by the data controller to close the integration control switch which commences the signal integration. A linear voltage ramp is formed by the signal integration of the DC waveform for the duration of the integration period. Thereafter, the signal is truncated at the terminal value of the ramp at the end of the integration time. Immediately, the voltage level accumulated across the integration capacitor is sampled and stored for subsequent transmission to the analog-to-digital (A/D) converter. On command, the data controller closes the dump switch which restores the integration capacitor to its reference level near zero volts, and awaits the next command from the data processor to commence the integrate-and-dump sequence. Commonly, the integration period is set by the length of time a scanning antenna takes to scan through its own beamwidth, or equivalently, by

the time required to scan through the diameter of its footprint projected on the earth. Typically, earth observations from instruments in orbit require a range of integration times, depending on the antenna beamwidths (or other criteria), ranging from 1 to several hundred milliseconds. The integrate-and-dump circuit integrates the signal information and produces an independent sample of the observed surface or target temperature during each integrate and dump period, viz., one integrate-and-dump period yields one degree-of-freedom in the estimation of the observed parameter. Naturally, there are many ways to implement the integration function; but, because integrate-and-dump circuits are so commonly employed in earth-orbiting instruments they are adopted here as a working example.

The data-controller block shown in Fig. 12 operates as a timer and organizer. It does not process data but operates to control the radiometer switching operations in such a manner as to produce a digital signal at the output that corresponds to the relative signal level of the blackbody target at the antenna. The true data processing segment of the observations is directed to a general purpose computer (not shown) or a microprocessor for this follow-on function. The computer or microprocessor may be aboard the spacecraft or receive information from the telemetry link at a ground station.

Typically, the output signal information from the receiver itself appears as a sequence of digital numbers whose relative numerical values correspond to target temperature variations at the collecting aperture of the antenna. The digital system in the data processor must be sized to respond to the total dynamic temperature range of the targets and to be consistent with the accuracy of the temperature measurements. The changes in the unprocessed digital numbers are explained by a mathematical temperature transfer function that is de-

signed, by reference to known target temperature changes, to infer the antenna temperatures of the observed targets and the intervening atmospheric constituents.

The data controller manipulates the switching functions within the radiometer to cause the warm and cold calibration loads to be (sequentially) observed within some defined time intervals during the observations. These calibration temperatures are programmed by the data processor to appear at the output terminals as relative digital-number magnitudes. Calibration temperatures thus observed are used to monitor the performance of the radiometer in such areas as calculating the temperature resolution, measuring the gain scale factor of the instrument, and participating as terms in a temperature transfer function to compute antenna temperature. As a practical example of the implementation of the digital number output levels, when the target temperature appearing at the collecting aperture of the radiometer is 300 K, the digital numbers are normalized to produce 3000 counts (digital numbers). Now when the collecting aperture views the cosmic background (2.7 K), the output may reduce to as few as 800 counts. By this observation the gain scale-factor is approximated by (3000 - 800)/(300 - 2.7) for 7.4 counts/K. In this example, the output response of the radiometer is referenced to the variations in the actual target temperatures and not to the temperatures viewed by the signal port of the modulator switch. For the same target temperature changes referenced to the signal input port the gain scale-factor would be considerably different, i.e., (3000 - 800)/(300 - 41.06) = 8.5 counts/K. The difference in the computation of the gain scale-factor, depending upon where the target temperatures are referenced, illuminates the importance of referring all operating temperatures to the same point to achieve a uniform understanding of the interpretation of the results. From this example it is clear that the critical com-

ponents of the operating radiometer reckon with the temperature changes that are separately referred to the input port of the modulator switch, that is, the transmission components, the mixer, the IF amplifiers, the ν-th law detector, and the video and digital equipment. For this reason the signal input port of the modulator switch qualifies as the true input terminal of the radiometer as an operating instrument. The circuits and components preceding the modulator switch serve mainly as transmission lines and calibration elements to service the input requirements of the operating radiometer.

The foregoing discussion illustrates that the RF transmission line components importantly impact and sometimes impose the limiting temperature variations viewed by the input to the radiometer. In this example the 2.7 K target temperature actually appeared as a 41.06 K source temperature to the radiometer input port. In fact, the dynamic range of the target temperature variations was reduced by an extent that could significantly impact the dynamic signal and noise relationships at the input to the ν-th law detector. In general, greater dissipative losses in the RF transmission circuits produce a larger compression in the range of the target temperatures at the signal port of the modulator switch. By comparison, it is interesting to compare the dynamic temperature range of the same targets at the input port of the total power radiometer at the feed aperture (Fig. 1). In the total power radiometer all the dissipative losses of the receiver components are referred directly to the feed aperture as the system noise temperature and the target temperatures (signal temperatures) are superposed on the system noise, without transmission losses or any temperature compressive effects. In this radiometer configuration, it is clear that the ν-th law detector must reckon with a wider dynamic range of signal temperatures (300 to 2.7 K, in this example) and in some instances the signal temperatures may more easily approach or exceed the noise

bias represented by the system temperature. With this consideration, the dynamic operation of the ν-th law detector is reasoned to be importantly different for the modulated and the total power cases, especially for target temperatures covering a wide dynamic range.

It is interesting to trace the signal and signal-to-noise relationships through the radiometer, given a specified change in the target temperature. For this purpose, assume that the RF component losses and their thermometric temperatures remain the same as the examples given in earlier paragraphs of this section, as referenced to the configuration shown in Fig. 11. Now consider the case where the target temperature T_{tar} is changed from 300 to 2.7 K--the cosmic background temperature. By the thermodynamic transfer of energy through the lossy RF components in the signal transmission line between the feed aperture and the input terminals of the receiver, this target temperature change of 300 to 2.7 K translates to a change in the input signal-to-noise ratio, T_{sig}/T_{sys}, from 300/422.83 = 0.71 (-1.49 dB) for the 300 K target temperature to $[(2.7/10^{\cdot 1/10}10^{\cdot 2/10}10^{\cdot 3/10}) + 38.711]/422.83$ = 41.06/422.83 = 0.097 (-10.127 dB) for the 2.7 K target temperature.

The corresponding output signal-to-noise ratio S_i/S_o for the 300 K target temperature is computed by substitution in (8) assuming τ = 0.126 seconds and that $B_{if} = 10^8$ Hz.

$$\frac{S_o}{N_o} = \left[\frac{\tau B_{if}}{4}\right]\left[\frac{T_{sig}^2}{\frac{T_{sig}^2}{2} + T_{sig}T_{sys} + T_{sys}^2}\right]$$

$$= \left[\frac{(0.126)(10^8)}{4}\right]\left[\frac{(300)^2}{\frac{(300)^2}{2} + (300)(422.83) + (422.83)^2}\right]$$

$$= 8.085 \times 10^5 \rightarrow 59.077 \text{ dB}$$

and for the 2.7 K target temperature by the same substitution in (8)

$$\frac{S_o}{N_o} = \left[\frac{(0.126)(10^8)}{4}\right]\left[\frac{(41.06)^2}{\frac{(41.06)^2}{2} + (41.06)(422.83) + (422.83)^2}\right]$$

$$= 2.7 \times 10^4 \rightarrow 44.31 \text{ dB}$$

Apparently, a temperature change in the target in the ratio of 300/2.7 = 111.11 (20.46 dB) produced a change in the signal-to-noise ratio at the input to the receiver of 0.71/0.097 = 7.32 (8.64 dB), which in turn produced a corresponding change in the signal-to-noise ratio at the output of the receiver of $(8.085 \times 10^5)/(2.7 \times 10^4)$ = 29.94 (14.76 dB). This example is given to illustrate quantitatively the propagation of the dynamic response of the target temperature change through the receiver in a typical operating configuration. One is counseled to note that the target temperature changes transferred to the input of the receiver are referenced to the system noise T_{sys}, and that the output signal response S_o is referenced to the output receiver noise N_o, which is most importantly reduced by the effect of the sampling statistics accumulated by τB_{if}.

Ultimately, one must reckon with the interpretation of the radiometer responses by the digital record it produces. In this example, we previously noted that for the existing internal gain-optimization-adjustments in the video

amplifier and in the A/D converter, a target temperature of 300 K produced a numerical value of 3000 digital counts and a 2.7 K target temperature produced 800 digital counts. Fully recognizing that the microwave radiometer is rigorously a statistical device, its performance must be interpreted in the argot of statistics. For this example, the 3000 digital count response to a 300 K target temperature is deduced by averaging many (about 50 or more) independent samples (degrees of freedom), as delivered by the integrate-and-dump circuits during the time that the feed aperture was viewing the target. The average value of the sample infers the signal component as produced by the target temperature, and the standard deviation about the signal mean infers the magnitude of the output noise level N_o. A sampling voltmeter measures both quantities.

The digital counts observed for the signal and the noise components can be converted into corresponding target temperatures and noise temperatures by division using the gain scale-factor as referenced to the input port or to the target, as desired. As an example, in one series of modulated radiometers operating in earth orbit, a target temperature of 300 K produces an average digital count of 3200 with a standard deviation of 5. The gain scale-factor for the particular radiometer channel, referenced to the input, is calculated to be 8.5 digital counts/K, which would estimate the output noise level to be $5/8.5 = 0.59$ K (1σ).

The temperature resolution for the example given here is estimated from (13) by

$$T_{sig} = \left[\frac{2\,T_{sys}}{\sqrt{\tau B}}\right]\left[1 + \frac{T_{sig}^2}{T_{sys}} + \frac{T_{sig}}{2T_{sys}^2}\right], \text{ K}$$

which by substitution of the computed quantities for a 300 K target temperature yields

$$T'_{sig}(300) = \left[\frac{(2)(422.83)}{\sqrt{(0.126)(10^8)}}\right]\left[1 + \frac{(300)}{(422.83)} + \frac{(300)^2}{(2)(422.83)^2}\right], \text{ K}$$

$$= [0.24]\ [1.96]$$

$$= 0.47 \text{ K}$$

and the temperature resolution at the 2.7 K target temperature is

$$T'_{sig}(2.7) = \left[\frac{(2)(422.83)}{\sqrt{(0.126)(10^8)}}\right]\left[1 + \frac{(41.06)}{(422.83)} + \frac{(41.06)^2}{(2)(422.83)^2}\right]$$

$$= [0.24]\ [1.10]$$

$$= 0.26 \text{ K}$$

Note that, here, T'_{sig} may be interpreted to mean the target temperature increment required to produce a change in the signal counts at the output equal to the equivalent noise counts at the output terminals of the radiometer.

A STATISTICAL INTERPRETATION OF TEMPERATURE RESOLUTION

A specification for the temperature resolution of a radiometric receiving system infers the level of its intrinsic noise as applied to the task of estimating the mean temperature of a specified external target. The temperature resolution, then, because of its noise level inference, operates to bound the available signal-to-noise ratio for a given set of measurements.

Consider, for example, a case where the thermometric temperature of seawater is to be estimated by an orbiting single-channel radiometer whose temperature resolution is specified at 0.6 K based on the available integration time

for the measurement and by the magnitude of the system-noise temperature (T_{sys}). In this example, a 1 K change is observed in the thermometric temperature of seawater, with the further knowledge that an emissivity of 0.2 is appropriate. The signal-to-noise ratio expectation for the 1 K change in the seawater measurement is then given as (1) (0.2)/0.6 = 0.33 (-4.8 dB) as bounded by the noise level as a limiting factor in the denominator, and for the change in the signal (seawater temperature change) in the numerator. Obviously, a temperature resolution specification of 0.6 K, for the measurement of seawater temperature variations in the vicinity of 1 K, is unsatisfactory because of the resulting negative signal-to-noise ratio. A successful observation with a satisfactory signal-to-noise ratio is therefore constrained to reduce the receiver noise...it is the only alternative left with only a single observing channel and with the observation time fixed. Signal-to-noise ratios exceeding 15 to 20 dB are typically needed to estimate the mean temperature of a target or its variations with high confidence (i.e., small confidence intervals).

In the argot of statistical inference, as applied to the determination of confidence intervals in an applied measurement, the properties of a population are estimated by a sample or by an ensemble of samples which operate either singly or in combination to improve the estimate of the population parameter. Consider the case where the true mean temperature u_t of a target is to be estimated by a sampling procedure. Consider further that the variance σ^2 of the target temperature is unknown. The point that is to be developed here is to show the structure of the functional form of the confidence interval for mean target temperature in its classical statistical form. Suppose, for example, that the measured properties of a radiometer yield the following quantities: T_{sys} = 800 K, B = 100 MHz, and τ = 0.125 seconds, where

T_{sys} is the system noise referred to the feed aperture (total-power configuration), B is the predetection bandwidth, and τ is the integration time for the measurement. Consider further that T_{sys} is the minimum noise level as bounded by the state-of-the-art of low-noise components and the transmission line losses, B is determined as a maximum value for the predetection bandwidth to limit the vulnerability of the radiometer to manmade interference, and that τ is the integration time which is constrained by the dwell time of the footprint during the antenna scan cycle. With these definitions and constraints the observation operates to produce the best possible signal-to-noise ratio. We note in passing that another look at the same target area (sea surface) is prohibited by the antenna scan pattern. The foregoing constraints on the variables are specified to illustrate that in many practical observations of the Earth's surface from orbit, the observation time for any one resolution cell (footprint) is severely bounded by practical operating conditions and that it is not possible to improve the signal-to-noise ratio.

Let us return to the task of estimating the mean temperature of a target that fills the beam of the feed aperture and with the further consideration that there are no other error media present such as target temperature instabilities, sidelobe contributions of the feed pattern, etc. With this model for the measurement we can write the expression for the estimation of the population mean target temperature u_t, where it is assumed that the mean target temperature is a population parameter which is to be estimated by a sampling procedure, and that the sampling procedure will produce the proper statistics to calculate the confidence intervals in the estimation of the mean target temperature.

u_t is estimated by

$$\bar{X}_t - t_\varepsilon \frac{s}{\sqrt{n-1}} \geq u_t \geq \bar{X}_t + t_\varepsilon \frac{s}{\sqrt{n-1}} \quad \cdots$$

with confidence intervals expressed about the sample mean $\bar{X}_t$

$$\bar{X} \pm t_\varepsilon \frac{s}{\sqrt{n-1}}$$

and with confidence factor t_ε, sample standard deviation s, and with n degrees of freedom τB.

Student's T-statistic t_ε is given as the confidence factor for the interval. When n, the number of degrees of freedom, exceeds about 120 and approaches infinity the magnitude of the confidence level $t_\varepsilon\, s/\sqrt{n-1}$ is interpreted to mean here that when $t_\varepsilon = 1$, 68% of the measured estimates of u_t are expected to lie within $u_t \pm (1)\, s/\sqrt{n-1}$ and that 95% of the estimates of u_t are expected to lie within $u_t \pm (1.96)\, s/\sqrt{n-1}$. When n assumes smaller values, Student's T-table should be consulted to provide the proper confidence factor.

In the practical application of the confidence intervals, s is construed to symbolize the standard deviation of the noise waveform in the predetection bandwidth, and n is specified by the number of independent samples reported every 1/B seconds for the duration of the integration period τ seconds.

From this commentary, the expression for the 1σ confidence interval for the estimate of the mean target temperature is reconstructed in equivalent forms

$$\pm \frac{s}{\sqrt{n-1}} \rightarrow \pm \frac{T_{sys}}{\sqrt{\tau B - 1}} \rightarrow \pm \frac{T_{sys}}{\sqrt{\tau B}}$$

which is readily recognized as the familiar expression for the temperature resolution.

In practice, n assumes very large values (>>120), and for this reason the numerical values of the confidence limits given above are appropriate. Because n is large it is convenient to drop the 1 under the radical. The confidence interval for the mean target temperature is mainly intended in this discussion to show the terms and factors that show its development and to illustrate its similarity to the familiar form of the expression for temperature resolution $T_{sys}/\sqrt{\tau B}$. What it does not express is the uncertainty (confidence limits) in the measurement of s. This consideration is developed in the paragraphs that follow.

In the system planning stages of a radiometric system the temperature resolution is calculated from best estimates (sometimes measurements) of the system noise T_{sys} for a prescribed range of predetection bandwidths and integration times. Usually these estimates of temperature resolution are reduced to equipment specifications which guide the development of the radiometric observing system to its completion.

The calculated estimate of temperature resolution and the measurement of the temperature resolution as an equipment parameter, however, are considerably different. In the planning estimates no allowance is given for the error in the measurement of T_{sys}. In the actual measurement of temperature resolution, T_{sys} operates as a statistical population parameter--namely, the standard deviation term s in the confidence intervals $s/\sqrt{n - 1}$. Because T_{sys} is a statistical quantity representing the standard deviation of the measurement, it has a confidence interval which conforms to the χ^2 (Chi-Squared) distribution function.

A proper statistical estimate of the temperature resolution of a radiometric system, when viewing a target at some particular temperature, requires that a sufficient number of independent measurements be taken to establish a confidence limit for the measurement of the temperature resolution itself.

A single point estimate, or a one-sample measurement (n = 1) of the temperature resolution, for example, is a meaningless quantity in statistical argot because it has no defined confidence limits to convey the reliability of the measurement or its repeatability. Yet it is a relatively common practice to state the measured temperature resolution based on a single measurement.

Consider a procedure where the temperature resolution is to be estimated at some specified target temperature based on the statistical fluctuations of the output signal waveform which is reasoned to represent the noise in the measurement. The mean value of the signal waveform fluctuations is proportional to the mean target temperature and the standard deviation of the statistical fluctuations about the mean represent the RMS noise, or as a measured parameter, the temperature resolution, T'_{sig}. When digital numbers are adopted to report the signal statistics of the measurement, each number is reported as the outcome of an estimate of the target temperature during the integration period.

An elaboration concerning the significance of a single digital number is given for clarity in the case of an integrate-and-dump type of circuit element which is subsequently converted to a digital number by an analog-to-digital converter. The digital number d_i in this example emerges from the signal-output data stream as a statistically independent sample (n = 1) for the estimate of the target temperature or to determine the noise component, which in this instance is defined as the temperature resolution. The temperature

resolution, when measured in this manner, is essentially an expression of the standard deviation of the statistical noise in the digital counts; it is calculated by the conventional expression for the standard deviation of sample size n.

$$s = T'_{sig} = \left[\frac{\sum_{i=1}^{i=n} (d_i - \bar{d}_i)^2}{n - 1} \right]^{1/2}$$

where $\bar{d}_i$ is the mean value of the digital counts.

At any time, s can be transformed from digital counts to temperature units by the application of the gain scale-factor (counts/K) for the system.

The measured result to express the temperature resolution is now in a form which will allow the determination of confidence limits for the measurement based on the sample size n.

As previously mentioned the χ^2 distribution is appropriate to determine the confidence limits for the standard deviation, or as in this example, the temperature resolution. The upper and lower confidence limits are given by the two-tailed confidence factors $\left(\chi^2_{a/2}, \chi^2_{-a/2}\right)$

$$\left[\frac{(n-1)s^2}{\chi^2_{(a/2,\, n-1)}} \right]^{1/2} \quad \text{and} \quad \left[\frac{(n-1)s^2}{\chi^2_{(-a/2,\, n-1)}} \right]^{1/2}$$

where n is the number of independent samples controlling the estimate of the confidence limit for the standard deviation. In the denominators of the confidence limits are expressed the confidence factors given by χ^2 tables for a specified confidence level--90% confidence levels are common in practice. It is convenient to note here that χ^2 is symbolically a mathematical function with an exponent of 2. Actually, it should be regarded as a single descriptive term where the squared superscript has no particular or practical significance.

An example to illustrate the foregoing discussion seems appropriate. Consider that an estimate of the temperature resolution T'_{sig} has produced a numerical value of 0.6 K with 20 independent samples. From a χ^2 table the tabular values for the upper and lower confidence limits based on n - 1 degrees of freedom (19) and for the 90% confidence limits yield

$$\left[\frac{(20-1)(0.6)^2}{10.12}\right]^{1/2} \quad \text{and} \quad \left[\frac{(20-1)(0.6)^2}{30.14}\right]^{1/2}$$

$$[0.82\ \text{K}] \quad \text{and} \quad [0.48\ \text{K}]$$

which, in statistical parlance, states that we are 90% confident that the true value for the temperature resolution T'_{sig} lies between 0.82 K and 0.48 K with only a 10% risk of being wrong.

COMMENTARY

This monograph investigates the basic operating principles of the total-power and modulated radiometer configurations. An effort has been made to explain the operation of these receivers to the level of detail needed to specify and qualify them for spaceborne operation. Wherever possible, terminology has been adopted that is most widely understood by the remote-sensing community at large. A number of examples are given with the express purpose of acquainting the reader with the practical processes and procedures that are encountered in the design of spaceborne radiometers.

Many definitions are given with the understanding that some have not been defined elsewhere; and for most, there is no universally accepted definition.

The material is structured to be tutorial in character...at times it is admittedly tedious. Nevertheless, the discussion is intended to convey the operating philosophy and the detailed technical considerations that affect the design of a successful spaceborne sensor.

REFERENCES

1. R. H. Dicke, "The Measurement of Thermal Radiation at Microwave Frequencies," Review of Scientific Instruments, Volume 17, Number 7, July 1946.

2. G. C. Southworth, "Microwave Radiation from the Sun," Journal of the Franklin Inst., 239, 285 (1945).

3. The temperature resolution specification expresses the operating sensitivity of the radiometer. The terminology for temperature resolution varies widely among the radiometer community and no serious effort has ever been launched to reach a uniform terminology or definition. Most commonly the term Delta-Tee is used to denote the change in antenna temperature required to produce some vague or undefined, observable output response from the radiometer. Other expressions such as noise-equivalent Delta-Tee (NEΔT), minimum detectable signal (MDS), noise equivalent power (NEP), 1σ noise, RMS noise, and others, have variously been used to express the same intent. For purposes of the material discussed here the term temperature resolution is adopted and is defined as follows:

   The temperature resolution is the change in the thermodynamic temperature of a blackbody enclosure, which totally contains the antenna radi-

ation pattern, that produces a signal-to-noise ratio of unity at the output terminals of the radiometer. With the further qualification that the postdetection bandwidth is much smaller than the predetection bandwidth. The temperature resolution is expressed as a 1σ statistic in kelvins.

4. The absolute temperature accuracy is defined here by two measured statistical quantities derived from the residual error matrix resulting from the measurement of the temperatures of standard blackbody targets whose accuracies are certified by the National Bureau of Standards over the total dynamic temperature range. The mean value of the measured residual errors expresses the expected accuracy of measurement and defines the magnitude of the systematic or bias error in the measurement. The standard deviation, s, of the residual errors expresses the precision of the measurement and the statistical scatter. The residual errors are defined as the measured differences between the standard target temperature and the corresponding temperatures estimated by the temperature transfer function for all target temperature measurements. The mean and standard deviation are expressed in kelvins. The 1σ confidence limits are typically given for the mean by $s/\sqrt{n-1}$ where n is the number of degrees of freedom contained in the matrix of residual errors. The confidence limits for the standard deviation are non-symmetrical and are best expressed by the Chi-Squared distribution. The confidence limits are frequently specified at the 90% level. Especially of note is that the absolute accuracy specification also contains the errors and imperfections of the temperature transfer function.

5. Antenna temperature is defined here as the thermodynamic temperature equivalent of the signal power appearing across the terminating resistance of the collecting aperture. The equivalence of antenna temperature and the power incident on the terminating resistance of the collecting aperture is conveniently related by the expression

$$P = \frac{h\nu}{e^{h\nu/KT} - 1} \quad , \text{ watts}$$

where h, ν, and K are Planck's constant, the frequency in hertz, and the Boltzmann Constant (joules), respectively, and where T is the temperature of the terminating resistance in kelvins; P is the incident power (energy) impressed upon the terminating resistance of the collecting aperture. By reciprocity, P is also equal to the power reradiated by the terminating resistance and redirected to the collecting aperture through the interconnecting transmission line.

At microwave wavelengths $h\nu/KT$ becomes very small and by substituting the power series expansion for $e^{h\nu/KT}$ the relationship for P and T reduces to the very good approximation

$$P = KT, \text{ watts/Hz}$$

6. Adapted from N. Stone and D. Middleton, "Full-Wave Detection of Signals in Noise," Cruft Laboratory Technical Report No. 182, Cruft Laboratory, Harvard University, Cambridge, Mass., August 1953.

7. W. H. Jordan, "Second Detectors," Chapter 7, Page 188: Microwave Receivers, Edited by S. N. Van Voorhis, McGraw Hill, New York, 1948.

8. S. J. Goldstein, Jr., "A Comparison of Two Radiometer Circuits," Proc. IRE, pp. 1663-1666, November 1955.

9. W. A. Johnson, "Effect of Modulation-Correlation Choices on Dicke Radiometer Performance," Proc. IRE, p. 1242, October 1964.

10. S. R. O'Donnell, "A Comparison of Radiometers," Master of Science Thesis, Ohio State Univ., 1963.

11. Project Cyclops, Appendix D: Square Law Detection Theory, Report No. CR 114445, Reviewed July 1973, NASA/AMES Research Center, Code LT, Moffett Field, California 94035.

12. D. F. Wait, "The Sensitivity of the Dicke Radiometer," Journal of Research, National Bureau of Standards - C. Engineering and Instrumentation, Vol. 71C, No. 2, April-June 1967.

13. The superheterodyne receiver, as illustrated in Fig. 5, operates with signal information entering the amplitude envelopes of both RF responses. When the signal information is characterized by blackbody radiation from a target, the signal is broadband and uniformly enters both of the RF responses. With the assumption that both RF responses are equal in area and gain, the double-sided noise figure is appropriate.

In a tuned-radio-frequency (TRF) radiometer, where the RF amplitude response is controlled mainly by the RF response of the amplifiers alone

there is no sideband response and the single-channel noise figure is appropriate. The noise temperatures relating the single-sided noise figures are given by

$$T_{ss} = 290\ (F_{ss} - 1),\ \text{kelvins}$$

$$T_{ds} = 290\ \frac{(F_{ss} - 1)}{2},\ \text{kelvins}$$

$$T_{ds} = T_{ss}/2,\ \text{kelvins}$$

where 290 K is the standard reference temperature to which all noise figure measurements are referred and where the subscripts refer to single- and double-sided notation. It is apparent that when noise figures are very large, the double-sideband noise temperature is about half that of the single-sideband noise temperature. When noise figures are low, however, huge errors can be made from this simple assumption.

14. Estimates for the measured value of the cosmic background temperature fluctuate slightly with time as more measurements become available and are entered into the statistics. During 1980, the cosmic background temperature was commonly adopted at 2.7 K with a 1σ uncertainty of 0.15 K at microwave wavelengths.